24. VARIATIONS IN THE CALCITE DISSOLUTION PATTERN ON THE BARBADOS RIDGE COMPLEX AT SITES 541 AND 543, DEEP SEA DRILLING PROJECT LEG 78A[1]

Christoph Hemleben and Anabelle Auras, Geologisch-Paläontologisches Institut, Universität Tübingen[2]

ABSTRACT

The calcite compensation depth (CCD) fluctuates as a result of changes in the water-mass system, thereby producing a distinct dissolution pattern. Differential dissolution changes the composition of the foraminiferal assemblages, reflecting the depositional environment in respect to the fluctuating CCD. The dissolution pattern for the comparatively shallow Site 541 on the Barbados Ridge indicates a depositional environment mostly above the CCD, but below the foraminiferal lysocline during the late Miocene to early Pleistocene. In contrast, sediments of the deeper-water Site 543 indicate a depositional environment above the CCD during the late Pliocene to early Pleistocene only. Furthermore, similarities in the dissolution pattern of corresponding time intervals of Site 541 (represented by superimposed faulted intervals termed Tectonic Units A and B) are recognizable. Sediments deposited clearly above the foraminiferal lysocline are rare.

INTRODUCTION

Since 1968, when the *Glomar Challenger* left Galveston, Texas for her first leg, the study of paleoceanography—the history of ancient oceans—has become most important. The reconstruction of time-varying parameters such as water chemistry, circulation pattern, fertility and distribution of organisms is one of the major objectives of paleoceanography. On the other hand, plate tectonics—the production and the subduction of oceanic crust—determines the paleogeography of the oceans. Since Leg 57 (von Huene, Nasu, et al., 1980), it has become obvious that subduction of ocean crust including the sediments is a highly complex process, which calls for more than one explanation. Previous Legs (e.g., Legs 60, 66, 67, respectively, Hussong, Uyeda, et al., 1982; Watkins, Moore, et al., 1982; and Aubouin, von Huene, et al., 1982) resulted in different models for the tectonic style of a modern convergent margin. The Leg 78A objectives were guided by those previous models in attempting to characterize the convergent margin of the Caribbean Plate at the Barbados Ridge complex (Figs. 1, 2). Intensive geophysical surveys suggested that both accretion and subduction were occurring simultaneously (Biju-Duval et al., 1978).

The intraoceanic arc of the Lesser Antilles islands is flanked in the west by the Grenada Trough and in the east by the forearc Barbados Ridge complex (Biju-Duval et al., 1978). The Atlantic abyssal plain underthrusts the Barbados Ridge complex to a distance of about 200 km (Tomblin, 1975) to the west at a rate of approximately 2 cm/y. (Fig. 2). Therefore, drilling sites were placed at the toe of the Barbados Ridge complex (Sites 541, 542), with reference Site 543 on the abyssal plain, just west of the deformation front (Fig. 2). The reference site penetrated 411 m of Quaternary to Late Cretaceous sediments overlying basaltic ocean crust. Drilling at Site 541 penetrated 459 m (and at Site 542, 325 m) of deformed Quaternary and Neogene sediments. Stratigraphic repetition and structural fabric of the cored sediments demonstrate the features of an accretionary prism. Off-scraped sediments of the down-going Plate pile up the sediments at Sites 541 and 542 (Moore, Biju-Duval, et al., 1982).

In this chapter we add more data to the history of the off-scraped sediments in comparison with those of reference Site 543 by looking into the faunal composition of the planktonic foraminiferal assemblages. Differential dissolution produces a distinct faunal composition pattern by which the most resistant species become enriched in the sediments, reflecting a fluctuating lysocline and calcite compensation depth (CCD).

METHODS

On board *Glomar Challenger*, normal samples of 10 cm^3 were taken and washed with a 10% solution of hydrogen peroxide (H_2O_2). In some cases a low-frequency ultrasonic bath was used for less than 5 s in order to clean the samples. Visual examination followed the drying procedure on board (see site reports, this volume). Shore-based work emphasized counting of species and calculating the Foraminiferal Dissolution Index (FDX). Whenever possible, 500 specimens were counted, from which the FDX was calculated, following Berger (1979a).

$$FDX = \Sigma (P_i R_i)/P_i$$

where P_i is the percentage of species, and R_i is the rank of resistance to dissolution of species i. The overall influencing factor R can be obtained either empirically by looking at the most resistant species in sediment samples (Berger, 1968, 1975; Biscaye et al., 1976; Parker and Berger, 1971) or experimentally as done by Sliter et al. (1975), Adelseck (1978), and Thunell and Honjo (1981). The results in Table 1 give comparative ranking lists of planktonic foraminifers with respect to their solution susceptibility (see also the annotated species list at the end of the chapter).

Because the small fraction (250–315 μm) is much more sensitive to dissolution, we used this fraction for calculating the FDX. The fraction >315 μm was used for correlation or in cases where the small fraction did not contain enough specimens to be counted. Therefore, the dissolution curve we obtained is mainly based on the FDX from the fine fraction, excluding the benthic foraminifers. Low FDX numbers indicate rather well-preserved samples, whereas high FDX numbers represent poorly preserved assemblages. According to our observations, a FDX of 4 is considered to represent an assemblage deposited at the lysocline level, because dissolution becomes noticeable.

[1] Biju-Duval, B., Moore, J. C., et al. *Init. Repts. DSDP*, 78A: Washington (U.S. Govt. Printing Office).

[2] Address: Geologisch-Paläontologisches Institut, Universität Tübingen, Sigwartstr. 10, D-7400 Tübingen, West Germany.

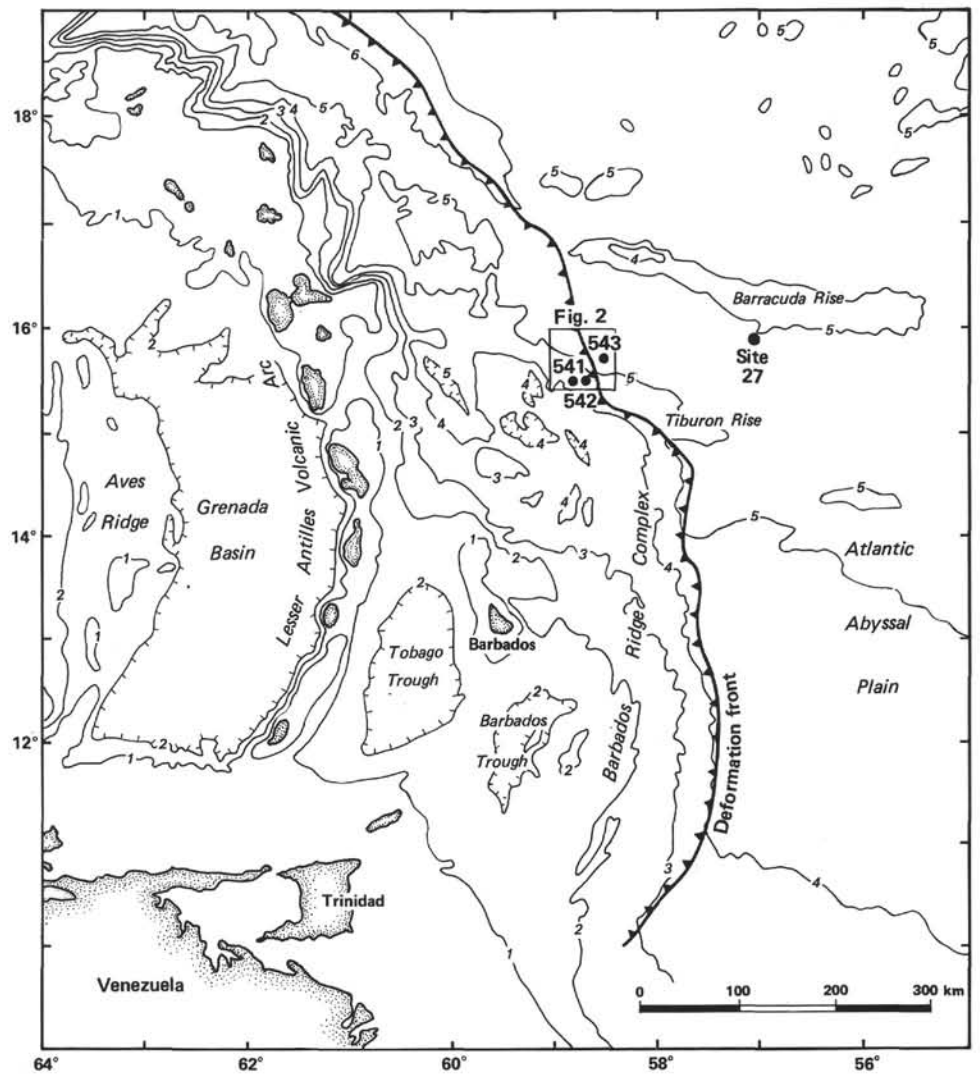

Figure 1. Regional location map; subduction front east of Barbados Ridge complex; water depth contours are in kilometers (adapted from Moore et al., 1982).

Table 1. Solution susceptibility ranking list of planktonic foraminifers including rank factor from delicate (1) to resistant (8).

Sediment ranking (Parker and Berger, 1971)	*In situ* ranking (Thunell and Honjo, 1981)	Laboratory ranking (Adelseck, 1978)	Sediment ranking (this chapter)	Rank factor (R)	Neogene species	Rank factor (R)
H. pelagica	*H. pelagica*	*H. pelagica*	*H. pelagica*	1		
G. ruber	*G. bulloides*	*G. aequilateralis*	*G. falconensis*	2		
G. aequilateralis	*G. aequilteralis*	*G. ruber*	*G. aequilateralis*	3	*G. praehirsuta*	4
G. sacculifer	*C. nitida*	*G. sacculifer*	*G. ruber*	3	*G. margaritae*	4
G. conglobatus	*O. universa*	*G. conglobatus*	*G. sacculifer*	4	*G. miocenica*	4
C. nitida	*G. menardii*	*P. obliquiloculata*	*O. universa*	4	*G. multicamerata*	4
O. universa	*G. sacculifer*	*S. dehiscens*	*G. conglobatus*	5		
G. truncatulinoides	*G. conglobatus*	*G. tumida*	*G. inflata*	5	*G. altispira*	5
G. inflata	*N. dutertrei*		*G. menardii*	5	*G. tosaensis*	6
G. crassaformis	*G. inflata*		*G. truncatulinoides*	6	*N. humerosa*	6
G. menardii	*G. truncatulinoides*		*N. dutertrei*	6	*N. acostaensis*	6
N. dutertrei	*P. obliquiloculata*		*G. crassaformis*	6		
P. obliquiloculata	*G. tumida*		*P. obliquiloculata*	7	*G. nepenthes*	7
S. dehiscens	*G. crassaformis*		*G. tumida*	7		
G. tumida	*S. dehiscens*		*N. pachyderma*	7		
			S. dehiscens	8	*S. paenedehiscens*	8

More or less monospecific samples produced by differential dissolution are considered to have been deposited at or close to the level of the CCD (FDX ≥ 7.5). In addition to the FDX obtained by counting, we considered several morphological features to be relevant to dissolution in questionable cases. These features are: (1) dissolved debris (chambers, keels), (2) pore widening, (3) absence or presence of calcite crust (Bé and Hemleben, 1970), (4) dissolved chamber surfaces, (5) occurrence of juvenile specimens, (6) thin last chamber, and (7) proportion of the sample fraction 250–315 μm (see Plates 1–2).

In addition, we used two reference samples from shallow depths (580 and 320 m water depth) off Barbados (Table 2). According to Berger (1979b) and Berger et al. (1982), virtually no calcite dissolution

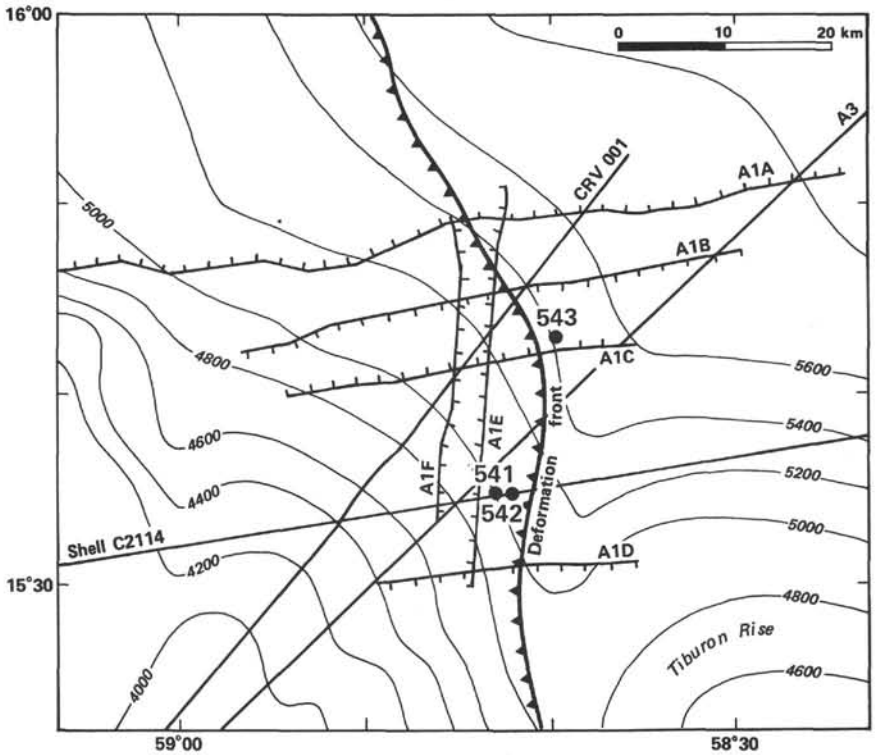

Figure 2. Site location map showing the position of the deformation front and seismic reflection profiles used for the site survey (adapted from Moore et al., 1982).

Table 2. Occurrence (%) and FDX of species in two reference samples from Recent sediments from 320 and 580 m water depths offshore Barbados in two fractions (μm) each.

	Sample BBD 320 m (%)		Sample BBD 580 m (%)	
	250–315 μm	>315 μm	250–315 μm	>315 μm
O. universa	1.2	2.0	0.2	4.6
G. conglobatus	—	1.2	0.4	8.6
G. ruber	60.0	28.4	56.8	16.6
G. sacculifer	25.8	32.0	27.4	21.0
S. dehiscens	—	0.2	—	—
G. falconensis	1.8	0.8	0.2	—
G. aequilateralis	3.0	2.2	2.2	0.6
N. dutertrei	3.8	23.4	8.8	32.6
P. obliquiloculata	—	0.8	0.2	2.0
G. truncatulinoides	0.6	1.2	1.6	2.4
G. crassaformis	0.4	0.2	0.2	0.4
G. menardii	1.4	7.6	2.0	11.2
Total	100.0	100.0	100.0	100.0
FDX	3.5	4.3	3.7	4.8

Note: The low FDX (excellent preservation) of the two reference samples demonstrate that, compared to other samples from much deeper environments (e.g., Sample 541-5-3, 19–21 cm—see Table 3), virtually no or only very little dissolution takes places while the tests are sinking from shallow to deeper water. — indicates no specimens were observed.

appears above the lysocline; whereas the lysocline can be defined as "a level of a sharp change in dissolution-rate gradient" (Berger, 1981). The lysocline for planktonic foraminifers must be placed empirically at more shallow depths that that for calcareous nannofossils (Berger, 1973a) or benthic foraminifers. The calcite compensation depth (CCD) "is the facies boundary between calcareous and noncalcareous sediments, noncalcareous being defined as a percentage below 10 and often close to zero" (Berger, 1981, p. 1442).

For identification of the planktonic foraminifers we used Blow (1969), Stainforth et al. (1975), and Brunner and Keigwin (1981). Additional sedimentological data were deduced from the core descriptions and photographs. For the SEM (scanning electron microscope) illustrations we utilized a rotation sputter unit and a Stereoscan 250 S.

As Site 541 was placed at the toe of the accretionary prism, the sediments were not only disturbed by drilling disturbances but also displaced by off-scraping. Therefore, we applied the stable isotope stratigraphy, the "*menardii-tumida* complex" (Schott, 1935; Ericson and Wollin, 1968), and the percentage of *G. ruber–sacculifer* for controlling the sequence (see also Oberhänsli and Hemleben, this volume). For the isotopic record of Sites 541 and 543 we studied samples of *Globigerinoides sacculifer, G. ruber, G. obliquus, Pulleniatina obliquiloculata*, and *Sphaeroidinella dehiscens* (Oberhänsli and Hemleben, this volume).

SITE 541

Introduction

Site 541 is situated at the edge of the Caribbean Plate right at the deformation front, at a water depth of 4940 m (Figs. 1, 2). Wright (this volume), places the calcite (carbonate) compensation depth (CCD) around 5200 m. Therefore, we estimate the foraminiferal lysocline to be at approximately 4800 to 4900 m. This estimation is corroborated by the assemblage observed in the first core liner (FDX = 4), which mostly contained seawater-suspended foraminifers from the seafloor or from sediments near the seafloor. The fauna can very well be compared with Recent reference samples well above the lysocline, taken off-shore Barbados at water depths of 580 and 320 m) (identified as BBD 580 m and BBD 320 m, respectively, Table 2).

Two major tectonic units (A and B) were cored at Site 541, separated by a reverse fault causing a major stratigraphic repetition: late Miocene mud overlies late Plio-

cene deposits (Fig. 3), dated with calcareous nannofossils (Bergen, this volume) and foraminifers. This horizon has been interpreted to result from undertrusting of pelagic sediments beneath the off-scraped deposits (Moore, Biju-Duval, et al., 1982). Other smaller repetitions occur in Cores 8 through 10 and 18 through 22 (Fig. 4). Hole 541 was continuously cored down to 460 m when the core barrel got stuck and the hole collapsed.

Tectonic Unit A (Hole 541)

Foraminiferal Assemblage Stratigraphy: Pleistocene

Tectonic Unit A represents late Miocene to Pleistocene sediments (Fig. 3) containing a tropical foraminiferal assemblage. Sediments of Cores 1 through 4 are strongly deformed by drilling disturbance. Cores 5 through 8 contain partially deformed sediments, whereas deeper cores contain more or less undisturbed sediments. Therefore, data derived from Cores 1 through 4 are of less value. Most samples show mixed assemblages of varying composition; the cause of the mixed assemblages is uncertain. However, a certain cold-water influence can be documented by the occurrence of *N. pachyderma* (right coiled), *G. inflata*, and *G. truncatulinoides*. The short interval, Sections 541-3-2 through 541-3-4, represents the best preserved assemblages (FDX = 4), indicating a depositional environment above the foraminiferal lysocline, demonstrated by the less resistant species *G. ruber* and *G. sacculifer;* approximately 70% of the fine fraction of Sample 541-3-2, 46–48 cm consists of *G. ruber* and *G. sacculifer* and another 18% are *N. dutertrei*. The coarse fraction is dominated by *G. menardii*.

Sample 541-4-6, 133 cm shows a distinct color change from light gray (carbonate-rich) to dark gray (carbonate-poor), which coincides with an abrupt faunal change; that is, a FDX change from 4 to 8. Sample 541-4-7, 8–10 cm again can be characterized by a FDX of 4. In addition, the assemblage of this short interval consists of only 78 specimens from a volume of approximately 3 cm^3 of sediment. This would indicate a depositional environment at or slightly below the CCD before being off-scraped. Change of color, abrupt faunal changes, and mud pebbles suggest that the sediments were displaced by a gravity flow. This hypothesis can be proved by the faunal composition, which shows *G. ruber* (var. pink) accompanied by keel fragments of *G. menardii*, a mixture of less resistant and resistant species.

From Core 5 downward, it seems to be possible to correlate the following sequence with Ericson's Stages Q to T (Ericson and Wollin, 1968) (or with Stage P to Q, of Briskin and Berggren, 1975).

The spike of excellent preservation (FDX = 4.0) in Sample 541-5-3, 19–21 cm may be assigned to Ericson's Stage U, the Illinoian (Riss) glacial period (Table 3).

The following Core 6 is mostly free of $CaCO_3$, indicating a dissolution maximum, that is, a preservation minimum or a high CCD level. This interval can be as-

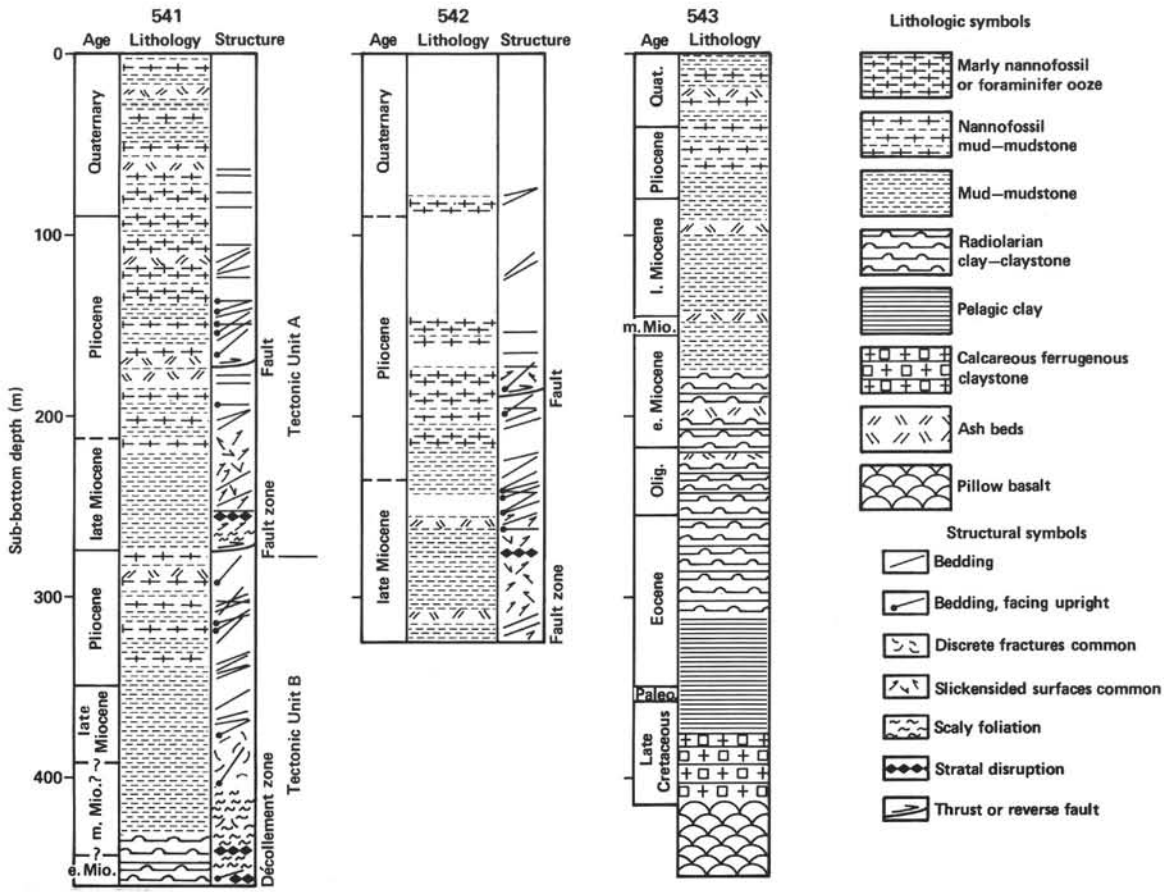

Figure 3. Lithostratigraphy and structural geology at Sites 541, 542, and 543 (adapted from Moore et al., 1982).

Table 3. Occurrence (%) and FDX of species in Sample 541-5-3, 19–21 cm.

	Fraction (μm)	
	250–315	>315
G. conglobatus	1.4	19.8
G. ruber	43.8	4.6
G. sacculifer	20.4	11.0
S. dehiscens	0.6	4.6
G. falconensis	5.8	—
G. aequilateralis	1.0	—
N. dutertrei	11.0	22.0
P. obliquiloculata	4.4	13.8
G. truncatulinoides	2.8	11.4
G. crassaformis	4.8	12.0
Benthic foraminifers	4.0	0.8
Total	100.0	100.0
FDX	4	5.7

Note: The low FDX of 4 indicates a depositional environment at or slightly above the lysocline. The percentages of species in the coarse fraction already indicate a slight enrichment toward the more resistant group. —indicates no specimens were observed.

Table 4. Comparison of species occurring in Sample 541-8-3, 141–143 cm and Section 541-8,CC.

	541-8-3, 141–143 cm (%)		541-8,CC (%)	
	250–315 μm	>315 μm	250–315 μm	>315 μm
O. universa	—	2.2	—	3.0
G. conglobatus	11.0	23.6	2.6	24.8
G. ruber	5.0	1.2	26.3	1.2
G. sacculifer	15.4	5.2	27.5	1.2
S. dehiscens	2.0	8.0	1.9	23.6
G. falconensis	0.2	—	0.6	—
N. dutertrei	41.2	17.4	25.0	14.8
P. obliquiloculata	19.8	38.0	5.8	2.0
G. truncatulinoides	2.8	3.8	—	—
G. crassaformis	—	0.6	2.6	4.2
G. menardii-G. tumida	—	—	7.1	24.8
Benthic foraminifers	2.6	—	0.6	0.4
Total	100.0	100.0	100.0	100.0
FDX	5.7	6	4.6	6.3

Note: This comparison shows the differences in the faunal composition in respect to the "*menardii-tumida* complex"; notice the presence of *G. truncatulinoides* where *G. menardii* is absent (compare with Fig. 4B). —indicates no specimens were observed.

signed to Ericson's Stage T, which, according to Briskin and Berggren (1975), has an approximate age of 535,000 to 996,000 y. This would be the Yarmouth or Mindel/Riss Interglacial. During this time, the "*menardii-tumida* complex" fluctuates at other locations (Ericson and Wollin, 1968), indicating several less prominent interglacials. At Site 541 only one small change can be observed between Samples 541-7-6, 110–112 cm and 541-7-4, 70–72 cm. The latter sample contains no *G. menardii* or *G. tumida*. Here, the question arises whether the earlier-mentioned Stage U really corresponds to Ericson's Stage U or represents a rather cold period during the Interglacial T. In the latter case, T would reach up to Section 541-2-1; this arrangement corresponds to the nannoplankton zonation (Bergen, this volume), but the very poor preservation of individuals of the mostly missing "*menardii-tumida* complex" argues against it (see the stratigraphic notes that appear later in the chapter).

The T/S stage boundary must be placed somewhere in Section 541-8-1, according to the fluctuation of the "*menardii-tumida* complex." This boundary coincides more or less with the nannofossil zone boundary *Helicosphaera sellii*/small *Gephyrocapsa*. Stage S, the Kansan or Mindel Glacial, ranges from Sections 541-8-1 through 541-8-6, despite its rather low FDX (= 6.0 of Sample 541-8-3, 141–143 cm). In contrast, Section 541-8,CC contains a high percentage of *G. menardii-G. tumida*, indicating the next older Stage R (Table 4).

Stage R, the Aftonian (Günz/Mindel) Interglacial, is represented by Sections 541-8-6 through 541-9-5, as indicated by a high percentage of *G. menardii*. According to Wilson (this volume), Core 8 belongs to the Matuyama reversed polarity interval. This is in agreement with our time scale. However, the Brunhes/Matuyama boundary should be correlated to the lower part of T. This again depends on whether T extends to the top of Section 541-5,CC or ends around Section 541-2-1.

The downward following sequence Sections 541-8-3 through 541-9-5 is a repetition of the nannofossil zones *Helicosphaera sellii* and *Calcidiscus macintyrei* (see Bergen, this volume) and corresponds to Sections 541-9-6 through 541-11-3. In our correlation this interval is equivalent to Stages S and R, but the upper part of Stage S (Section 541-9-5) is missing. This absence can be noticed within Sample 541-9-5, 115–145 cm. Sample 541-9-6, 25–27 cm belongs to Stage S, as indicated by the presence (12%) of the cold-water species *G. inflata*.

Stage Q is documented by the sediments of Sections 541-10-6, approximately 100 cm, through 541-11-2, approximately 100 cm. The Pliocene/Pleistocene boundary itself, as defined by the first appearance of *G. truncatulinoides*, can be placed within the interval between Sample 541-11-3, 131–132 cm and the top of Section 541-11-4. This is in contrast to the determination based on nannofossils by S. Bergen (this volume), who places the boundary between Samples 541-11-2, 75–76 cm and 541-11-3, 75–76 cm.

Stage P, defined by Briskin and Berggren (1975) as the first appearance of a "*menardii*" peak in the Pleistocene, could not be detected in the Pleistocene. However, the interval just below the Pliocene/Pleistocene boundary (Bergen, this volume), Samples 541-11-4, 0–2 cm to 541-11-4, 35–37, contains up to 30% *G. menardii* and *G. tumida*. Thus the first peak of the "*menardii-tumida* complex" falls within the latest Pliocene at Site 541. This is more comparable with Ericson and Wollin's (1968) Core V 12-18 of the South Atlantic than their Core V 16-205 of the central equatorial Atlantic. In addition, the Olduvai event was detected between Sections

541-11-2 and 541-11-3, above the *menardii* peak (Wilson, this volume).

The stable isotope record (Oberhänsli and Hemleben, this volume) reflects the same difficulties resulting from drilling disturbance that we also had in interpreting the FDX in Cores 1 through 4 (and partially 5). Nevertheless, the early Pleistocene Stages P to T can be identified by comparing the ^{18}O data with those of Core V 16-205 from the Central Atlantic Ocean (van Donk, 1976).

The comparison of *G. ruber* and *G. sacculifer* abundances with the oxygen isotope signal suggests a change of the water-mass system as well as changing salinities rather than temperatures. During Stage R (lower section) we observe high *G. ruber* abundances and relatively light ^{18}O values. This would indicate water lenses with low-salinity seawater, possibly drifting northward. In contrast, during the upper part of Stage R the high abundance of *G. ruber* coincides with relatively heavier ^{18}O values, indicating an expansion of the southern Sargasso Sea with higher salinity concentration into the Caribbean (Oberhänsli and Hemleben, this volume).

This observation can be compared with the situation today in which lenses of low-salinity seawater (~32‰ salinity) pass Barbados during the summer (Steven and Brooks, 1972). The winter and early spring season can be characterized by a southern Sargasso Sea assemblage with rather highly saline water (~36‰ salinity) comprising *G. truncatulinoides, G. aequilateralis*, and *G. ruber.*

We summarize our observations as follows: (1) Cores 1 through 4 are too much disturbed by drilling for any realistic interpretation. (2) The "*menardii-tumida* complex" reflects the climatic changes; therefore, Cores 5 through 11 can be assigned to Ericson's Stages Q–T, or Stage P of Briskin and Berggren (1975); alternatively Core 5 can be assigned to Stage U. (3) Thus the late Pleistocene cannot be recognized positively; it may be totally missing. (4) The fluctuation of carbonate preservation reflects the changing CCD level and runs mostly parallel to the climatic changes (Berger, 1979a). (5) In addition, the oxygen isotope signal and the abundance of *G. ruber* and *G. sacculifer* signifies the climatic trend, indicating changes in the water-mass system. (6) Comparisons with magnetostratigraphy and nannofossils suggest that the Matuyama/Brunhes boundary occurs somewhere in Core 6, above the nannofossil zone boundary *Helicosphaera sellii/Pseudemiliana lacunosa* Zone. (7) One major repetition occurring in Cores 9 and 10 could be recognized by a repetitive dissolution pattern in Core 10. (8) The first peak of the "*menardii-tumida* complex" occurs in the uppermost Pliocene just below the Pliocene/Pleistocene boundary.

Foraminiferal Assemblage Stratigraphy: Pliocene–Miocene

The late early Pliocene to late Pliocene can be characterized by two main intervals of rather well-preserved foraminiferal assemblages: (1) Sections 541-11-4 through 541-14-6 and (2) 541-14,CC through 541-17,CC. Each interval demonstrates only one time of poor preservation: Samples 541-12-2, 8–10 cm and 541-15-5, 128–130 cm (the latter is shown in Table 5). Most other samples show an excellent to moderate preservation (FDX = 4.5).

During the late Pliocene the "*menardii-tumida* complex" can be characterized by the dominance of *G. multicamerata*, which begins in Core 14. Minor constituents of the assemblage are the rather delicately shelled *G. miocenica* and some *G. menardii* and *G. tumida.* In summary, these species emphasize the rather warm and stable period of the late Pliocene. However, a remarkable change in species composition exists in the interval from Samples 541-12-6, 8–10 cm through 541-13,CC. These samples contain mostly very well-preserved assemblages without any species of the "*menardii-tumida* complex"; the preservation can be compared with Ericson's Stage S, indicating a low position of the CCD. The interval may be interpreted as the beginning of the climatic fluctuation that characterizes the Pleistocene. Abundant *G. sacculifer* indicates a rather high—or normal—seawater salinity, possibly derived from the southern Sargasso Sea.

The aforementioned intervals (from Sections 541-11-4 through 541-14-6, and 541-14,CC through 541-17, CC) are highly influenced by frequent gravity flows, well documented in Sections 541-13-5 and 541-13-6: alternating layers, rich and poor in foraminifers, which coincide with color changes of light to dark gray. Samples taken from these light gray layers reveal species sorted by gravity flows. In addition, the samples differ by carbonate content in respect to their size fractions. In agreement with Berger's (1971) settling ranks from fast to slow (*S. dehiscens, N. dutertrei and N. acostaensis, G. sacculifer, G. ruber*, and *O. universa*), we observed *O. universa* enriched in the upper two-thirds and *S. dehiscens* enriched in the lower third. In general, the state of preservation of single specimens is better in these samples, because they were buried rather rapidly by gravity flows; or the assemblage composition does not agree with the common trend. For example, thin-shelled *G. ruber* should not occur together with keels of *G. menardii* and many fragments of different species (Fig. 4A, Sample 541-4-3, 58–60 cm). Therefore most of the gravity flows exhibit a rather high FDX. In addition, shallow-water benthic foraminifers are missing in the gravity

Table 5. Fluctuations of the FDX of two samples, representing the dissolution pattern during the late Pliocene.

	Sample 541-14-4, 138–140 cm (%)		Sample 541-15-5, 128–130 cm (%)	
	250–315 μm	>315 μm	250–315 μm	>315 μm
O. universa	0.2	3.0	0.9	19.7
G. conglobatus	1.8	3.8	2.8	18.7
G. ruber, G. obliquus	32.3	7.0	5.9	3.9
G. sacculifer	20.3	14.4	5.5	5.2
S. dehiscens, S. paenedehiscens	5.0	30.4	51.2	33.3
G. falconensis, G. bulloides	—	—	1.3	0.3
G. aequilateralis	0.4	—	0.2	—
G. altispira	27.6	18.4	7.3	6.2
N. acostaensis	10.2	1.4	18.5	3.6
G. multicamerata, G. miocenica	1.0	14.4	1.8	3.9
G. praehirsuta, G. scitula	1.0	0.8	1.3	—
G. crassaformis	—	—	2.0	1.6
Benthic foraminifers	0.2	0.4	1.3	3.6
Total	100.0	100.0	100.0	100.0
FDX	4.4	5.5	6.5	5.6

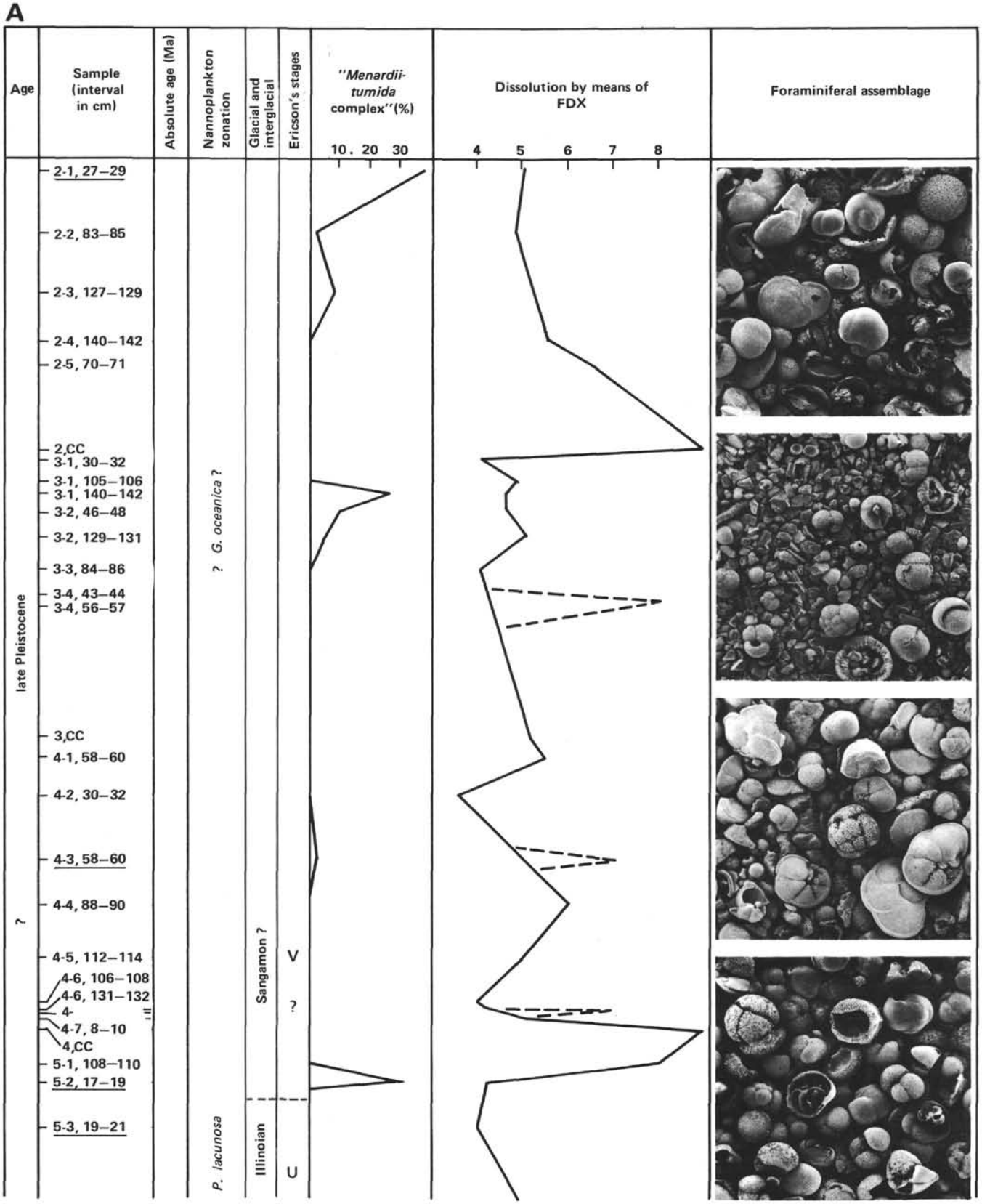

Figure 4. A–I. Combined stratigraphy (late Miocene to Pleistocene) and dissolution index of foraminiferal assemblages of Site 541; underlined samples correspond with the photographs in foraminiferal assemblages column; short dashed spike refers to an assemblage influenced by a gravity flow; dashed line refers to a microfossil-barren interval; dotted-dashed line refers to an interval that has not been investigated; all figures are magnified ×150.

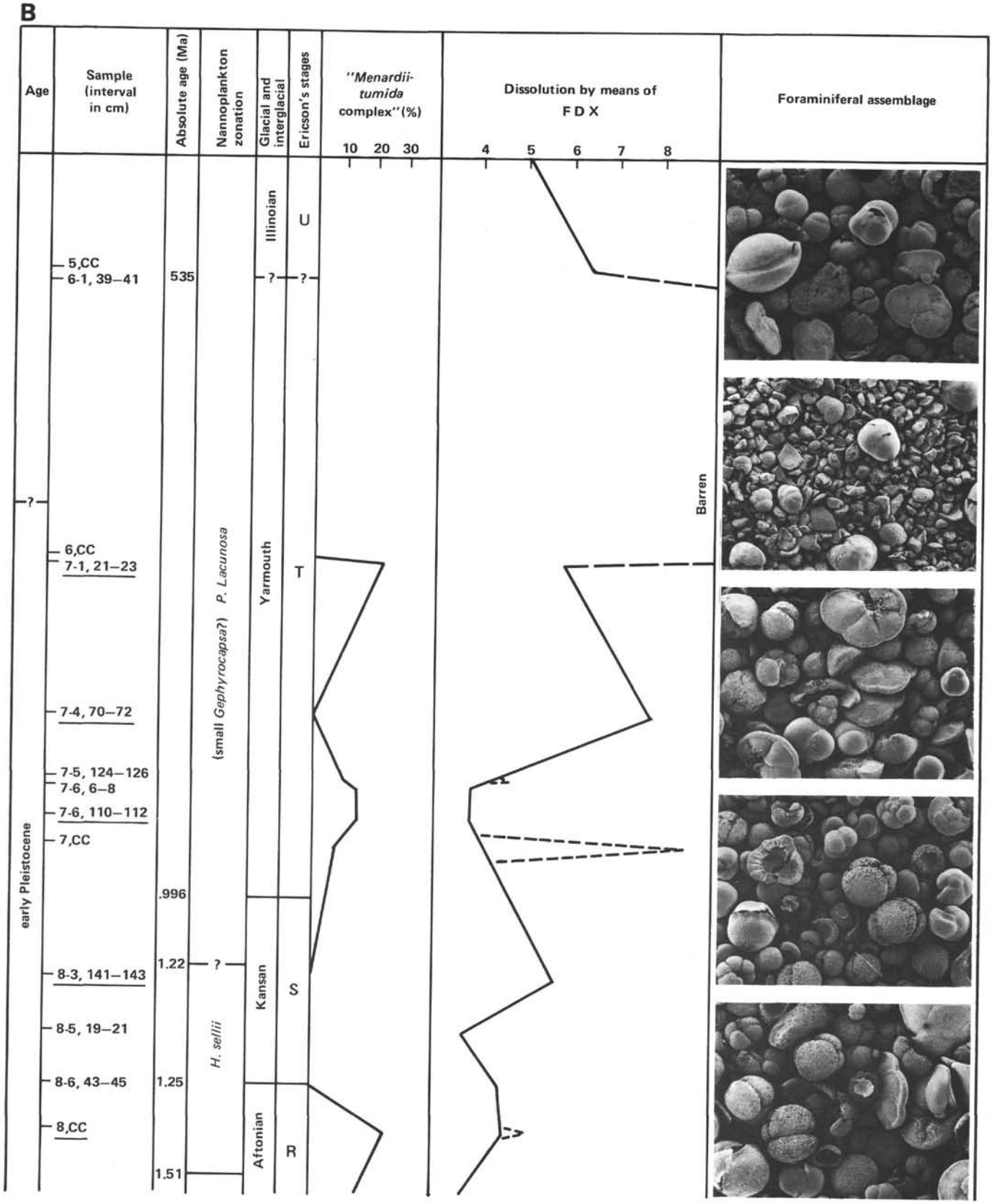

Figure 4. (Continued.)

C

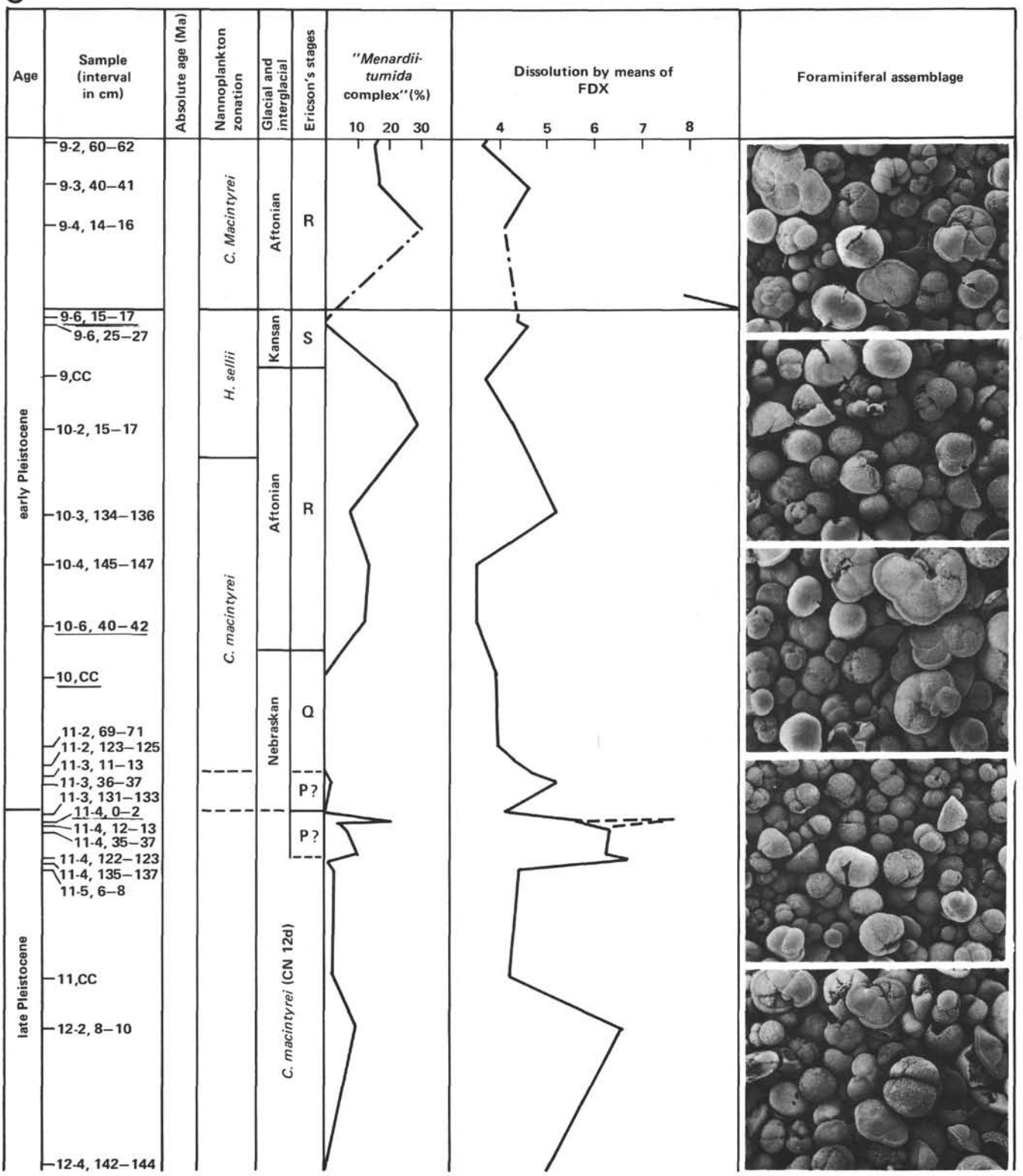

Figure 4. (Continued.)

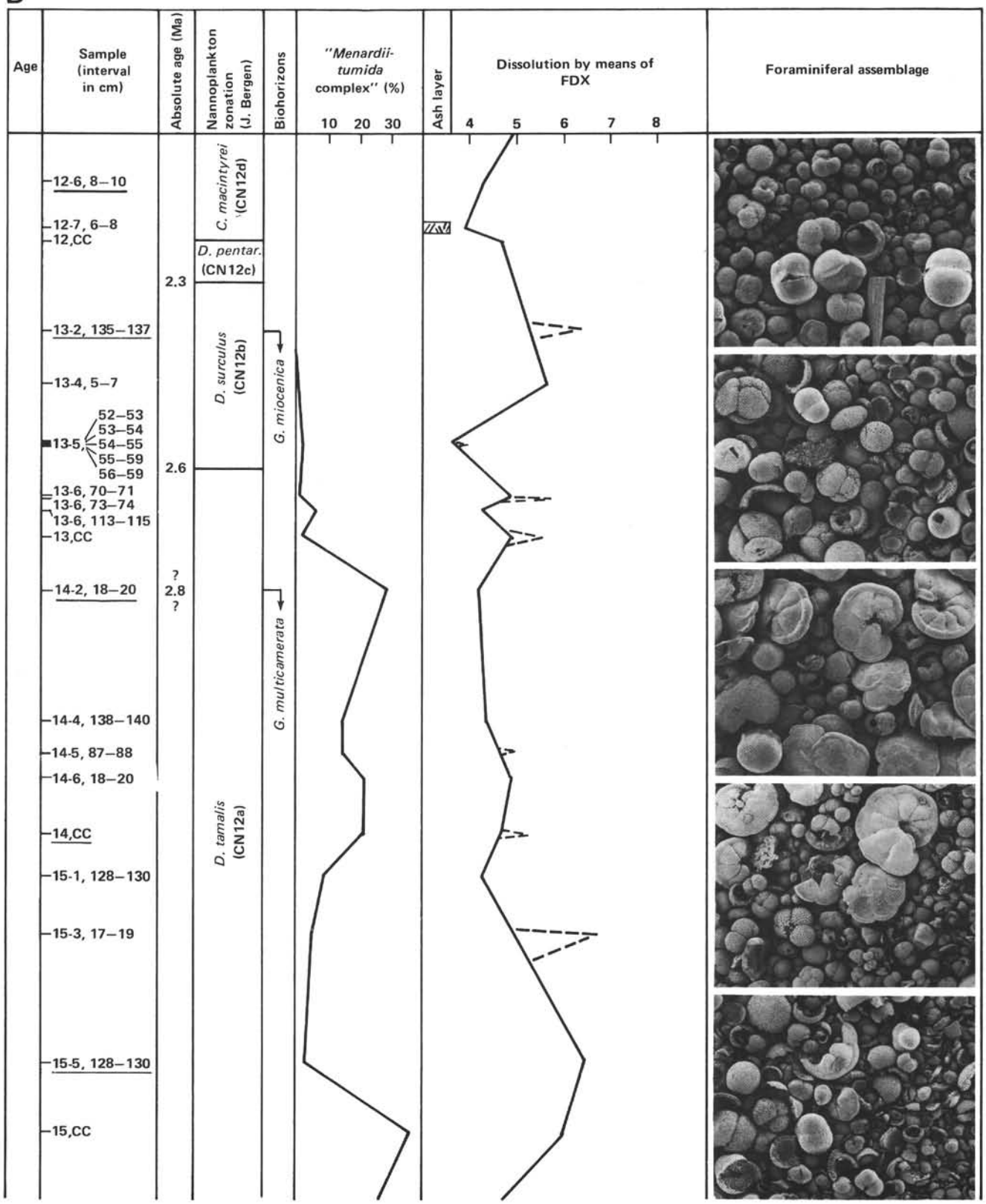

Figure 4. (Continued.)

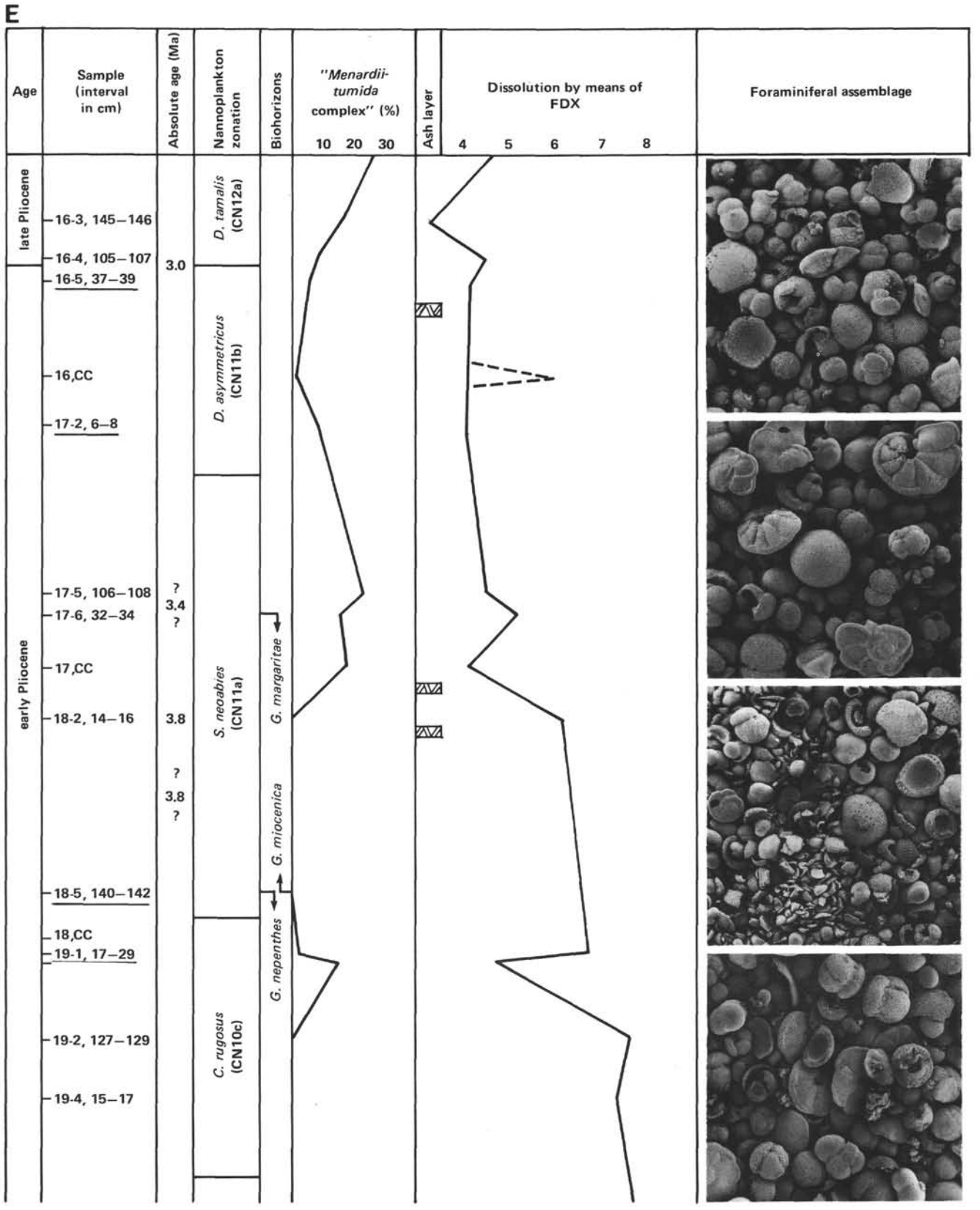

Figure 4. (Continued.)

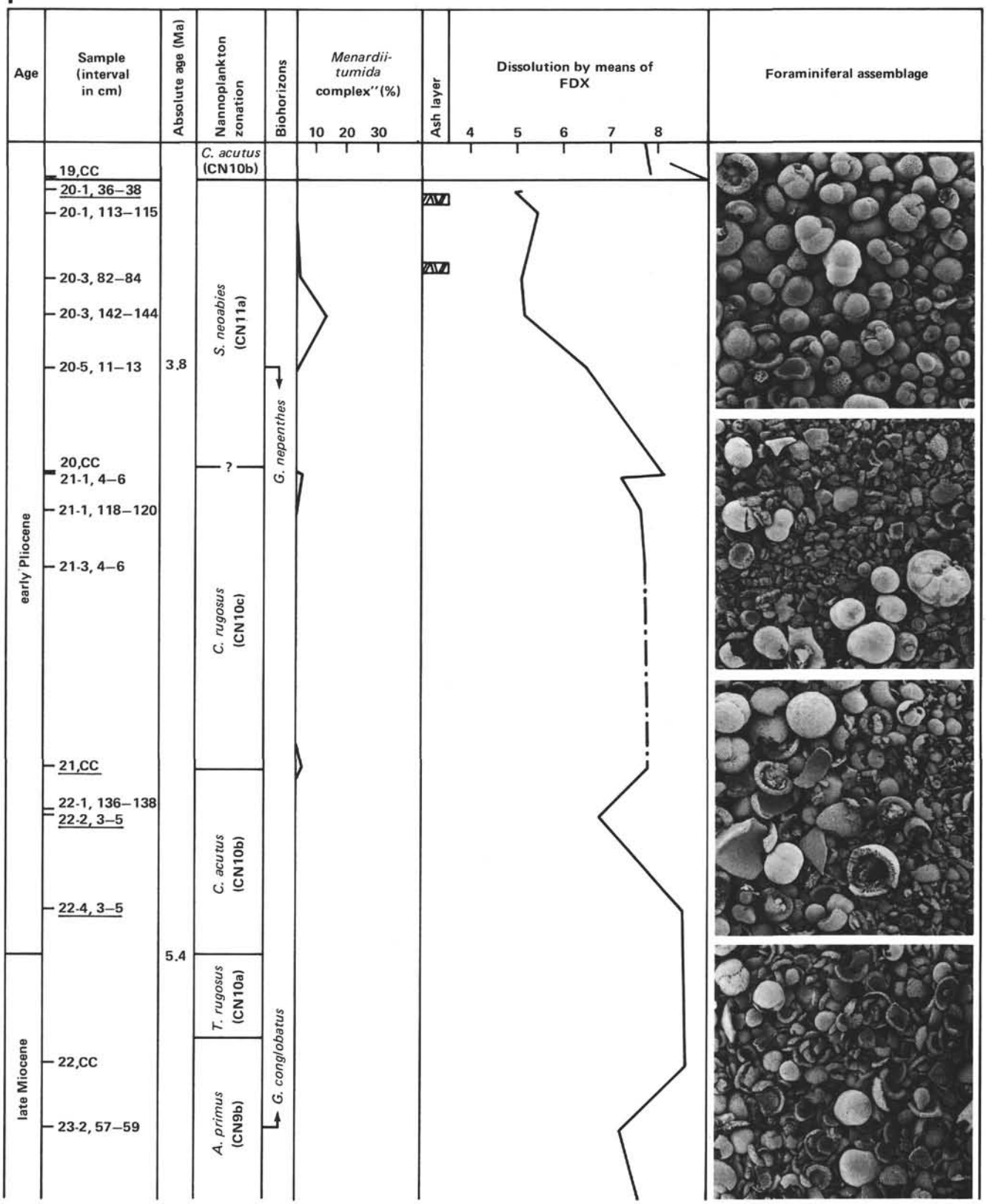

Figure 4. (Continued.)

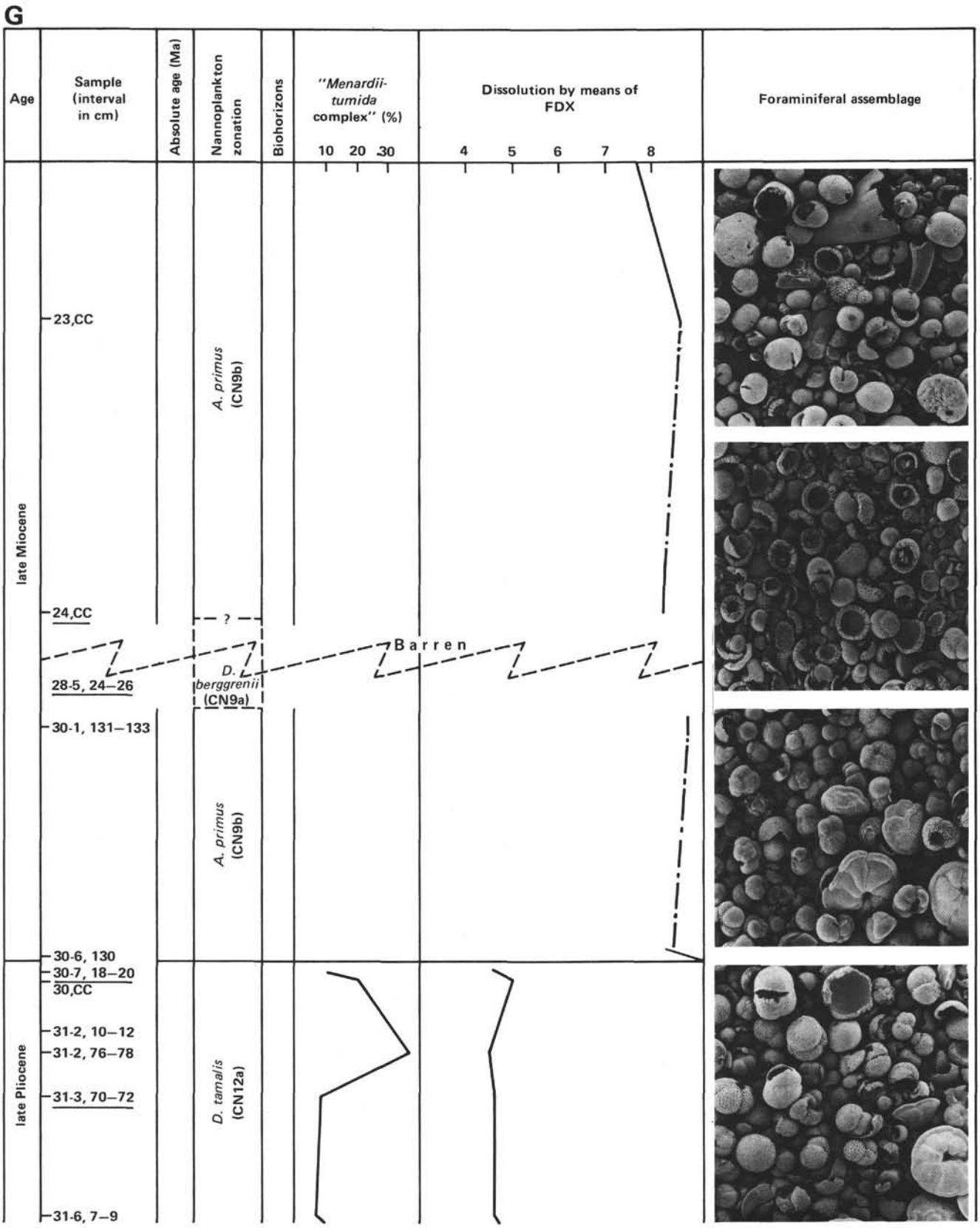

Figure 4. (Continued.)

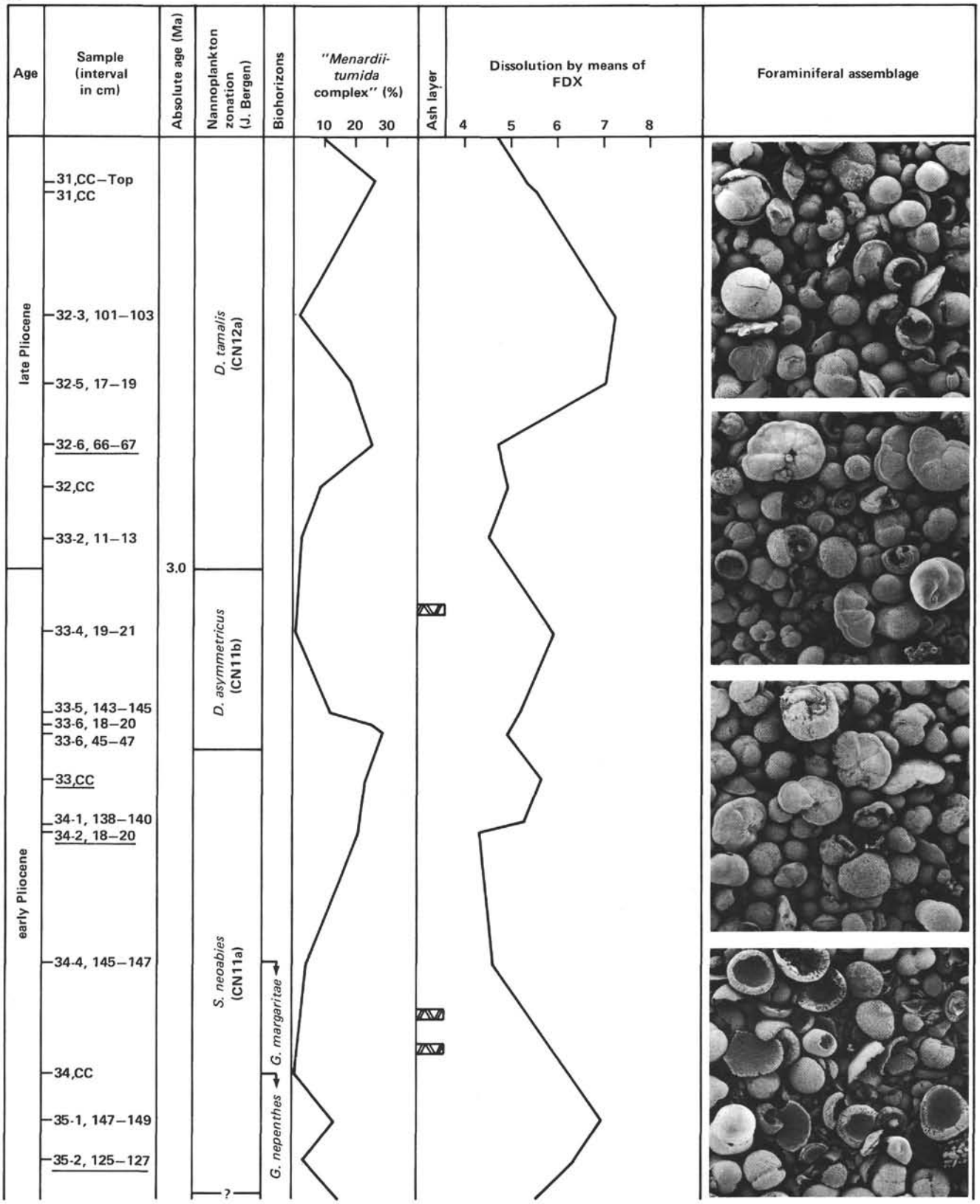

Figure 4. (Continued.)

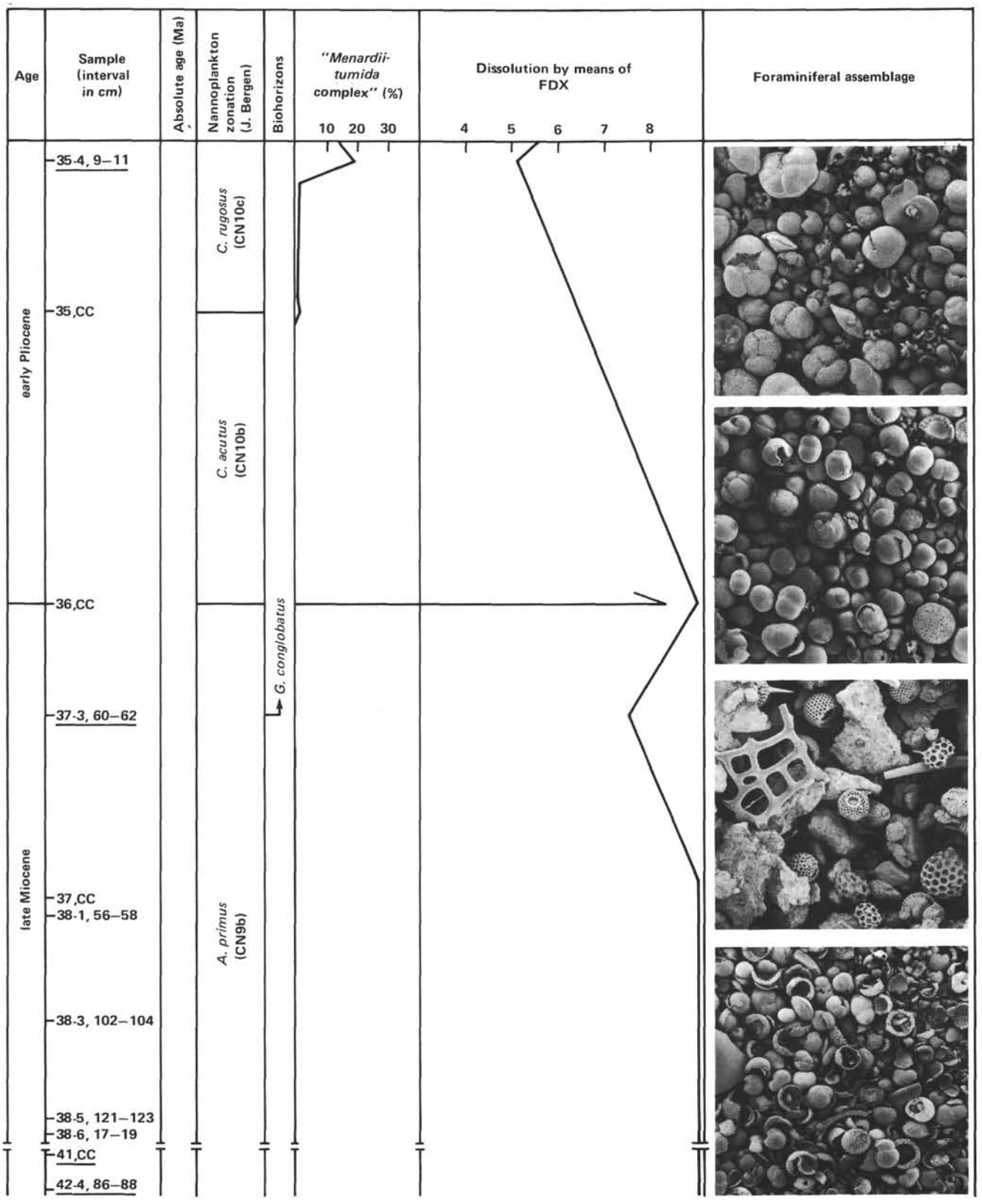

Figure 4. (Continued.)

flows except sparsely distributed fragments. This indicates an origin for the gravity flows from outside of the continental slope area, but within the Barbados Ridge complex; thus transport did not occur over long distances, but mostly from higher regions, as indicated by the preservation.

In general, we can very well differentiate the gravity flows from the normal sedimentation if the original layers are present. However, it is very difficult to make this distinction when gravity flows are deposited at the CCD and are subsequently bioturbated (Plate 3, Fig. 1). On the other hand, if we imagine an oscillating CCD accompanied by normal sedimentation, the sedimentary pattern of light and dark layers (Plate 3, Fig. 2) may reflect small climatic changes (see Oberhänsli and Hemleben, this volume).

The oxygen isotope record indicates for the same interval (Cores 541-14 through -16) pronounced isotopic excursions towards heavier values (Oberhänsli and Hemleben, this volume). This may indicate that we are seeing the time when the Northern Hemisphere ice sheet formed, well documented by Shackleton and Opdyke (1977) around 3.2 Ma.

Farther downward, beginning with Sample 541-18-3, 14–11 cm, the fluctuations of the "*menardii-tumida* complex" (including *G. multicamerata*) become obvious, probably representing the time when Northern Hemisphere glaciation began. Furthermore, this coincides with the last occurrence of *G. margaritae* in Sample 541-17-6, 32–34 cm. Sample 541-18-5, 140–142 cm marks the extinction of *G. nepenthes*, which agrees very well with the first normal event in the Gilbert reversed epoch around 3.8 Ma (Wilson, this volume).

The tectonic repetition reported by Bergen (this volume) in Cores 18 through 22 can be seen in the foraminiferal assemblages but is not clearly verified by the preservation. Because these cores were deposited at or close to the CCD, further correlations are difficult to draw (see the stratigraphic notes at the end of the chapter). Nevertheless, correlations between magnetostratigraphy, nannoplankton zonation, and foraminiferal occurrence exhibit some incongruities that occur in the repetitive sequence. According to the nannofossil zonation (Bergen, this volume), the Pliocene/Miocene boundary can be placed between Samples 541-22-4, 22–23 cm and 541-22-5, 22–23 cm. Core 23 contains foraminiferal debris and some tests of *S. paenedehiscens* and *G. conglobatus*, whereas *S. dehiscens* does not yet appear. Thus Sample 541-23-2, 57–59 cm can be assigned to the topmost part of the late Miocene.

Core 541-24 contains only few calcareous benthic foraminifers, indicating a depositional environment below the CCD but rather close to it. Cores 25 through 27 lack any carbonate. In contrast, Core 28 contains a foraminiferal assemblage consisting of the most resistant forms like *S. paenedehiscens* or *G. nepenthes*. Core 29 contains some calcareous nannofossils and benthic foraminifers only; they are concentrated by differential dissolution, which has been noted by previous workers (e.g., Parker and Berger (1971); Schnitker (1979) on Leg 48). The same is true for Hole 543A, where we were concerned with the CCD level during the Late Cretaceous (Hemleben and Troester, this volume). According to the nannofossil zonation, Core 28 through Section 541-29-3 can be assigned to CN9a *(Discoaster berggrenii)* overlying CN9b *(Amaurolithus primus)* of Sections 541-29-4 through 541-30-6. This repetition cannot be seen in the foraminiferal assemblages, because most samples are barren.

Core 541-30 again (Section 541-3-1 through 541-30-6, 128 cm) contains some foraminiferal debris of no diagnostic value. In conclusion, in the Miocene a fluctuating CCD rose slowly, leading to deposition of mostly carbonate-free sediments.

Summarizing our data, we may conclude that most Miocene sediments of Sections 541-22-4 downward were deposited below the CCD, as calcareous fossils are mostly missing. The occurrence of few and poorly preserved nannofossils does not prove any depositional environment above the CCD. Redeposition and sediment mixing by burrowing animals can always preserve a certain amount of carbonate. In addition, the samples demonstrate the different susceptibility to solution of planktonic foraminifers, benthic foraminifers, and calcareous nannofossils. If we assume little or no subsidence during the Pleistocene, we have to expect, according to Berger and von Rad (1972), a rising CCD toward the Miocene. This is inaccordance with previous work by Berger (1973b) and Berger and Winterer (1974).

Beginning with the early Pliocene, in Core 18, the CCD oscillates around the seafloor. The late to late early Pliocene is rather balanced and only interrupted by two periods of poor preservation. The onset of the climatic glacial–interglacial fluctuations is recorded in the latest Pliocene (starting around 2.6 Ma) in Core 13. The stable isotope record at Site 541 demonstrates the same trend (Oberhänsli and Hemleben, this volume). Shackleton and Opdyke (1977) reported from the Pacific equivalent data showing the beginning of these fluctuations in the later Gauss anomaly around 2.7 Ma.

Tectonic Unit B (Hole 541)

Foraminiferal Assemblage Stratigraphy: late Pliocene–late Miocene

Sediments of Tectonic Unit B are more consolidated, diagenetically altered, and possibly more bioturbated; therefore, assemblages of this unit are generally less well-preserved than comparable ones of Tectonic Unit A. In addition, sediments of this unit seem to have been deposited in deeper water than those of the overlying sequence (Fig. 5).

Sample 541-30-6, 133–135 cm exhibits fault planes of an underthrusting slab of middle Pliocene calcareous mud (Moore, Biju-Duval, et al., 1982). The mud contains late Pliocene assemblages comparable with those of Sections 541-14-2 through 541-16-4. The preservation minimum in Sample 541-32-3, 107–109 cm can be compared with that in Sample 541-17-5, 128–130 cm and in 541-34,CC with 541-18-2. In contrast, Sample 541-34-2, 18–20 cm contains a very well-preserved assemblage with a FDX = 4.3, comparable with Sample 541-17-5,

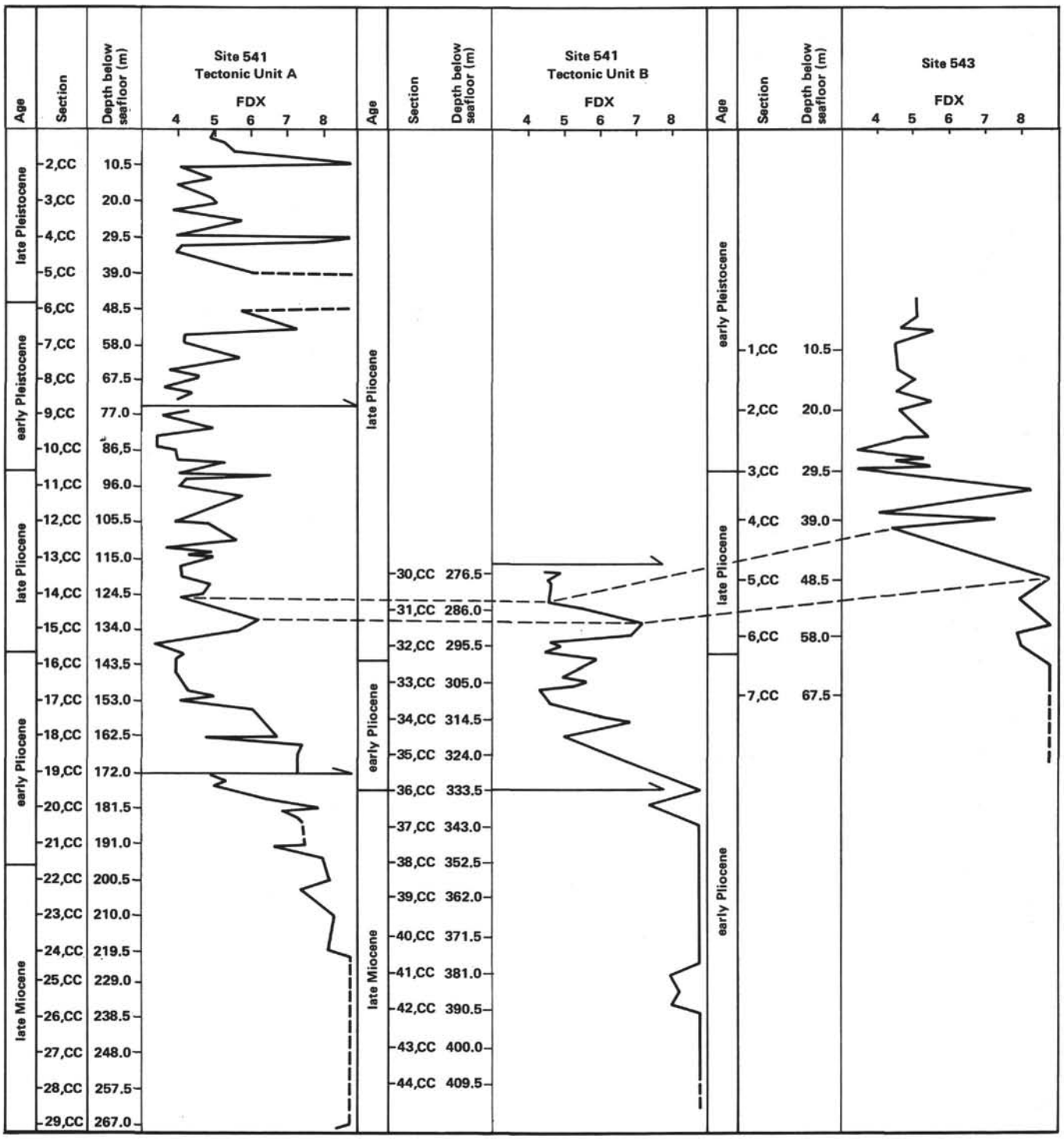

Figure 5. Preservation of foraminiferal assemblages as indicated by the FDX from Miocene through Pleistocene at Site 541 (Tectonic Units A and B) and Site 543. Notice similar dissolution patterns (FDX is between approximately 4 and 7.5) in both tectonic units, indicating a depositional environment mostly in the compensation zone. The FDX of Hole 543 for the Pliocene indicates a depositional environment at the CCD level. Arrows mark the faults; the dashed lines give an example of corresponding dissolution levels; stratigraphic boundaries based on the nannoplankton zonation are partially adopted from Bergen (this volume).

106–108 cm. Juveniles, as well as thin-shelled specimens, are present, indicating a depositional environment above the lysocline in both cases. However, comparisons of the FDXs in both intervals show a mean FDX around 4.0 in Unit A, whereas the underthrusting sediments contain less carbonate, with a mean FDX of about 5. Despite this minor difference, the preservational as well as the stratigraphic record is equivalent in both intervals. This similarity indicates a rather undisturbed sequence in both units. In contrast, the interval from Sections 541-20-1 through 541-22-2 does not really coincide with the overlying sequence, but seems to be derived from a deeper environment.

In upper Miocene sediments (Cores 37 downward), the samples contain only very little carbonate, not enough for further stratigraphic determinations by foraminifers. However, because *G. conglobatus* is present in Sample 541-37-3, 60–62 cm, this interval can be assigned to the topmost part of the late Miocene or to a more recent age. Samples 541-41-6, 33–35 cm and 541-42-4, 86–88 cm contain, besides *G. nepenthes* and *S. dehiscens*, only foraminiferal debris. Nannofossil zones can be detected down to Section 541-42,CC, which can be assigned to the *Discoaster berggrenii* Subzone (CN 9a) of Okada and Bukry (1980) (Bergen, this volume). However, the fluctuating occurrence of some calcareous determinable fossils points toward a slowly rising, oscillating CCD. Cores 43 through 46 are mostly unfossiliferous. One exception occurs in Sample 541-45-1, 11–13 cm, which contains some benthic foraminifers and fragments of planktonic species. The radiolarians appear first in Sample 541-41,CC, then increase in number and species in the downward-following cores. The appearance of radiolarians indicates a depositional environment well below the CCD.

In summary, we conclude that the Pliocene–Miocene sequence of Hole 541 of the underthrust unit (Tectonic Unit B) is quite comparable depositionally and stratigraphically to the overlying section, but may have been deposited in slightly deeper water than the corresponding interval of Tectonic Unit A. Furthermore, a similar dissolution pattern can be recognized in both units by comparing the corresponding intervals (Fig. 5).

SITE 543 (Hole 543)

Foraminiferal Assemblage Stratigraphy: Pleistocene

The reference Site 543 is positioned on the Atlantic abyssal plain, approximately 3.5 km east of the deformation front. Hole 543 was drilled in a water depth of 5633 m, about 400 m below the local CCD (Wright, personal communication, and this volume). Consequently, the top of Core 1 contains only few specimens or fragments of planktonic foraminifers. Furthermore, drilling disturbance seems to prevent any reliable results. Nevertheless, the combination of the calculated FDX, the counts of the "*menardii-tumida* complex," and stable isotopes indicate, throughout the cores, certain trends that are combined in Fig. 5. The nannofossil zonation established for Site 543 by Bergen (this volume) was of some assistance to us in placing the *Helicosphaera sellii/Pseudoemiliania lacunosa* Zone boundary near Sample 543-1-4, 120 cm (Fig. 6). This means the interval from Sections 543-1-4, 120 cm through 543-3,CC belongs to the early Pleistocene. In other words, Ericson's Stages Q (P of Briskin and Berggren, 1975) through T are represented in Sections 543-1-2 through 543-3,CC (Table 6).

The Pliocene/Pleistocene boundary can be placed between Section 543-3,CC (by nannofossils) and Sample 543-4-1, 120–122 cm by planktonic foraminifers. Comparisons with Site 541 show a similar dissolution pattern, especially for Stages R, S, and the lowermost part of T. The preservation minimum of Stage T demonstrated at Site 541 seems to be missing or destroyed by drilling disturbance. The interval corresponding to the lower R and Q stages shows more variation compared with Site 541. However, the "*menardii-tumida* complex" exhibits rather comparable fluctuations. Stage Q can be determined by the lack of *G. menardii–G. tumida*, and Stage P by the presence of this group in accordance with Site 541. Nevertheless, the first peak of the "*menardii-tumida* complex" (Section 543-4-1) falls within the uppermost Pliocene or cuts across the Pliocene/Pleistocene boundary. The boundary, determined by nannofossils, falls within the sample interval 543-3,CC and 543-4-1, 54–55 cm; however, the first appearance of *G. truncatulinoides* can be observed in Sample 543-4-1, 120–122 cm; this matches the situation of Site 541.

Summarizing the results, it becomes quite obvious that (1) the late Pleistocene is missing at reference Site 543. This may also explain the possibly missing late Pleistocene in the off-scraped sediments at Site 541. This is also true for Site 542, according to the nannofossil stratigraphy. (2) Ericson's stages Q through lowermost T (or P of Briskin and Berggren) are represented by Core 543-1 through Section 543-4-1. (3) The first "*menardii-tumida* complex" peaks below the Pliocene/Pleistocene boundary, as Bergen has determined (this volume).

Foraminiferal Assemblage Stratigraphy: Pliocene

The Pliocene sequence of Hole 543 demonstrates a still deeper depositional environment than at Site 541, Tectonic Units A and B (Fig. 5). Lower Pliocene to Miocene sediments were deposited well below the CCD, as indicated by carbonate-barren cores. Beginning with Core 17, radiolarians occur with increasing abundance and persist downward to include Core 34 (332 m subbottom) of the lower Eocene. This core of Hole 543 cor-

Table 6. Correlation between absolute age, Ericson's stages, and core intervals, demonstrating the missing late Pleistocene in Hole 543.

Absolute age interval (Ma) (Briskin and Berggren, 1975)	Ericson's stage boundaries	Approximate interval
0.996	T/S	543-1,CC to 543-2-1
1.250	S/R	543-2,CC to 543-3-1
1.565	R/Q	543-3-5, 29 cm to 543-3-5, 100 cm
1.630	Q/P	
1.752	Pliocene/Pleistocene boundary	543-4-1, 120–122 cm

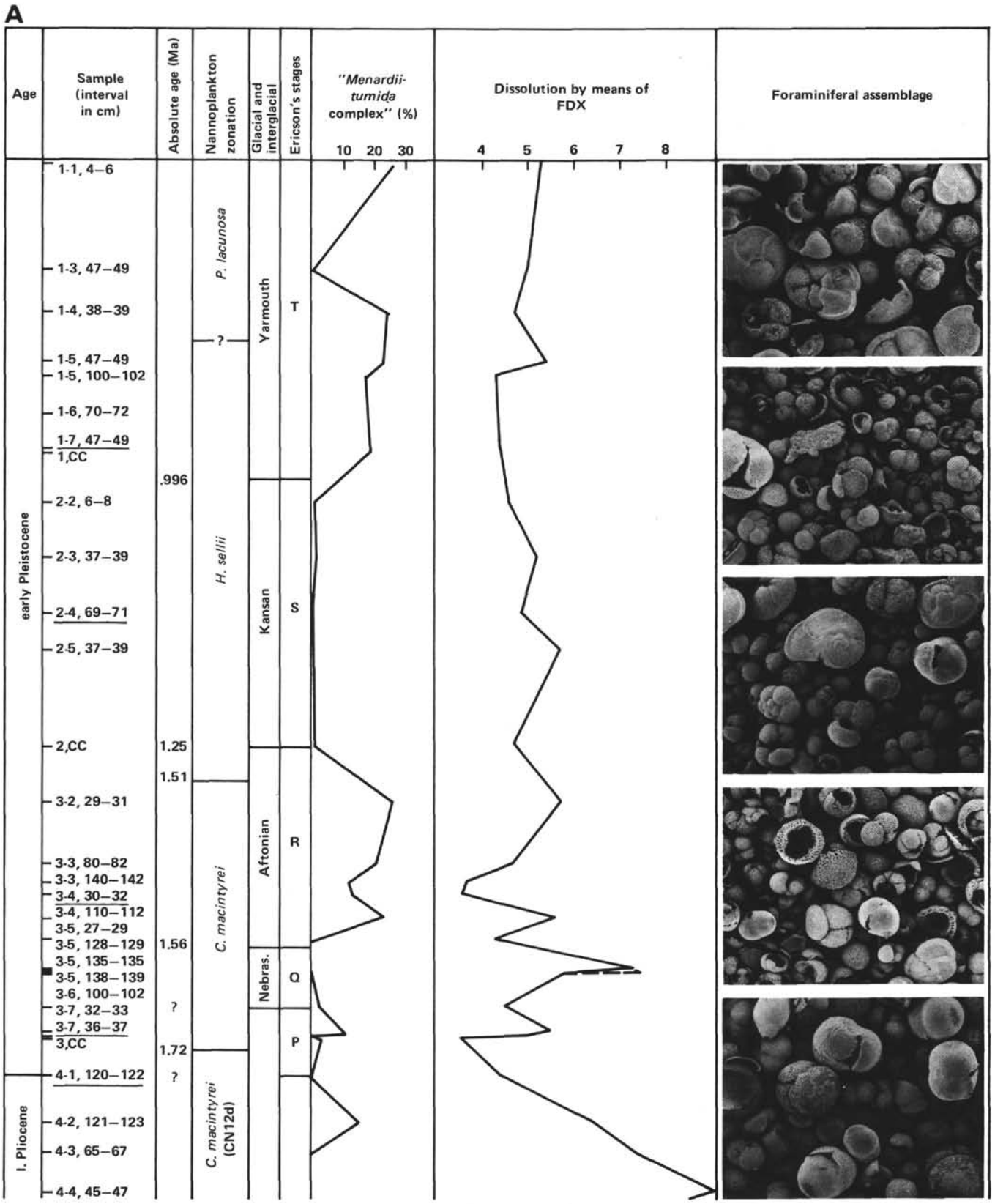

Figure 6. A–B. Combined stratigraphy (Pliocene–Pleistocene) and dissolution index of foraminiferal assemblage of Hole 543; underlined samples correspond with the photographs in foraminiferal assemablages column; dashed spike refers to an assemblage influenced by a gravity flow; all magnifications are ×150.

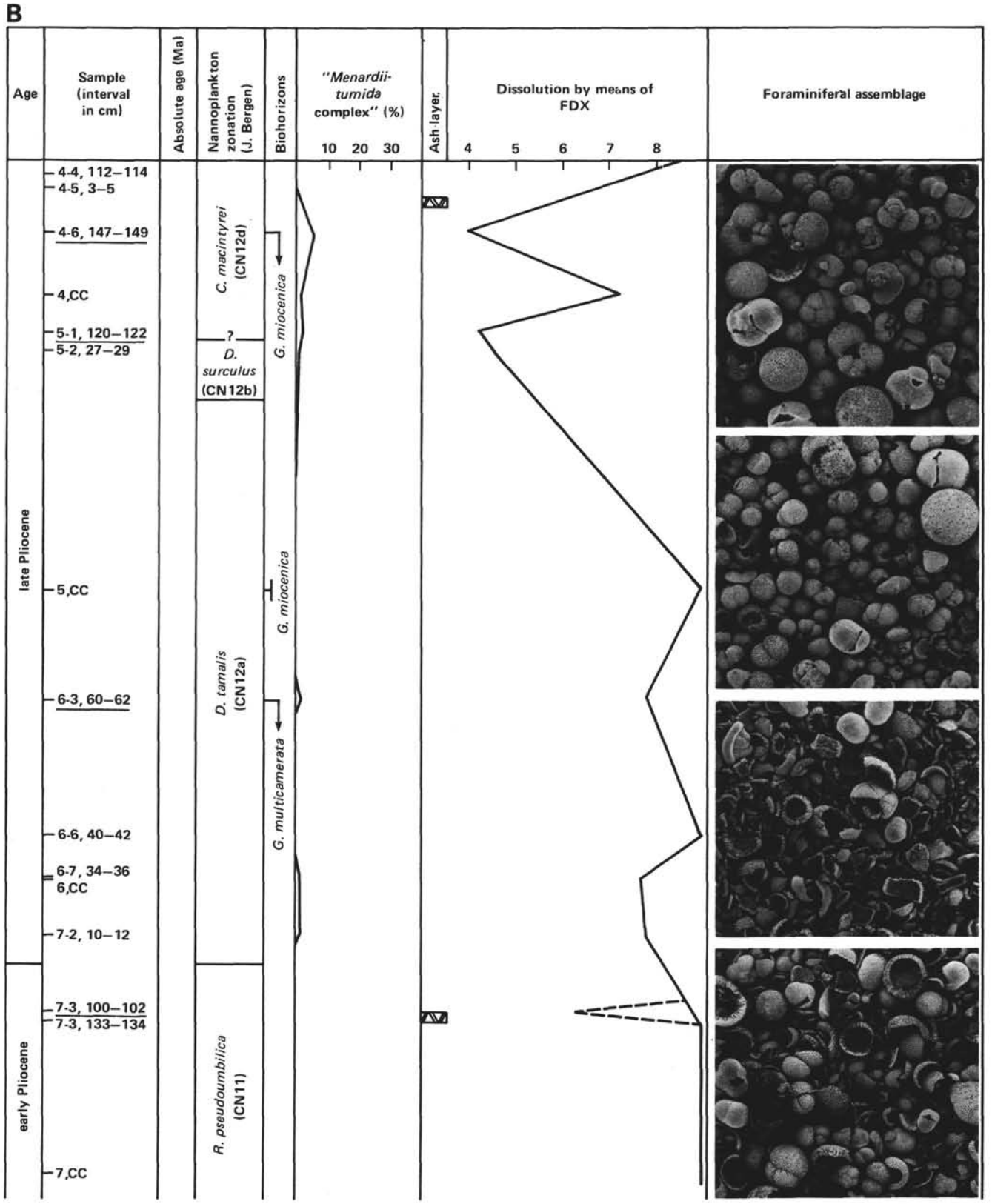

Figure 6. (Continued.)

responds to Core 2 of Hole 543A (see Hemleben and Troester, this volume). Comparisons of the FDX with Site 541, Units A and B, are rather difficult. The reasons for this are (1) rather wide-spaced sampling, (2) poor preservation of the assemblages, and (3) difficulties in stratigraphical correlations (e.g., the stratigraphy based on nannofossil correlations shows a hiatus in the middle late Pliocene). Nevertheless, a tentative correlation can be made (Table 7).

In addition, the ash layer in Sample 543-7-3, 115 cm corresponds to the ash layers in Samples 541-16-5, 140 cm and 541-33-3, 135 cm; this is the interval after the extinction of *G. margaritae* and *G. nepenthes*. Furthermore, Sample 543-8-2, 90 cm corresponds to Samples 541-18-1, 140 cm, 541-20-1, 105 cm, and 541-34-5, 75 cm. This should be approximately the datum level of the extinction of *G. margaritae* around 3.4 to 3.5 Ma (Table 8).

CONCLUSION

The preservation of planktonic foraminiferal assemblages, demonstrated by the FDX, is a useful tool for tracing the foraminiferal lysocline and the CCD. The fluctuation of these levels is closely related to climatic changes, especially during the Pleistocene. The FDX of Pliocene assemblages of Tectonic Unit A in Hole 541 can be very well compared with those of Tectonic Unit B, although the latter unit was deposited in a slightly deeper environment than Unit A (Fig. 5). Thus the offscraped sediments originate from a shallower depth, for example, the Tiburon Rise east of the deformation front.

Sediments of the reference Site 543 on the Atlantic abyssal plain northeast of the deformation front were deposited in still deeper water, as indicated by the FDX (Fig. 5). Thus a detailed comparison between the FDX of Pleistocene assemblages of Site 543 with 541 is rather difficult. The "*menardii-tumida* complex" reflects the climatic change more accurately than does the FDX curve. Consequently, it became very difficult to use Site 543 as a reference site for the purposes of careful paleoceanographic reconstruction.

In summary, we see that most sediments of Site 541 were deposited during the late Miocene through early Pleistocene above the CCD, but below the lysocline. In contrast, the sediments of Site 543 indicate a depositional environment above the CCD only for the late Pliocene through late Pleistocene. Furthermore, only very few intervals at both sites indicate a depositional environment clearly above the foraminiferal lysocline. Locally, however, gravity flows have carried some few but excellently preserved specimens below the CCD. From the detailed analysis we can deduce that sediments of the late Miocene to early Pliocene were mostly deposited close to the CCD or even below it, which may indicate a rather warm period around 4.7 to 4.3 Ma. Since then the decreasing FDX may reflect a certain cooling during the late early Pliocene and early late Pliocene. The beginning fluctuation of the "*menardii-tumida* complex" (including *G. multicamerata*) suggests climatic changes independent of the dissolution pattern. This fluctuation coincides with changes in the circulation pattern of the water masses that resulted from the beginning of Northern Hemisphere glaciation around 3.0 to 2.6 Ma.

The late Pliocene was characterized by even more pronounced fluctuations and disturbances by gravity flows, indicating a higher carbonate production and/or certain tectonic movements. The FDX of early Pleistocene assemblages and the "*menardii-tumida* comlex" reflect rather accurately the changing water-mass systems during the different glacial and interglacial phases. Thus Ericson's Stages Q (or Stage P of Briskin and Berggren) through T are recognizable.

Table 7. Corresponding dissolution levels of Hole 541, Tectonic Units A and B, and of Hole 543.

Hole 541, Unit A (core-section)	Hole 541, Unit B (core-section)	Hole 543 (core-section)
14,CC	31-5	5-2
15-3	32-2 to 32-3	5,CC

STRATIGRAPHIC NOTES

We adopted the nannoplankton zonation mainly from S. Bergen (this volume). Because several inconsistencies appeared during our study, we tried to correlate our findings with paleomagnetic data supplied by Wilson (this volume) and with time scales published by Briskin and Berggren (1975), Gartner (1977), Okada and Bukry (1980), Brunner and Keigwin (1981), and from a personal communication (W. A. Berggren, 1981).

Quaternary

The position of the Pliocene/Pleistocene boundary varies according to the method being used. Here the boundary has been defined by the first appearance of *G. truncatulinoides*. At *Site 541*, the early Quaternary sequence of Cores 6 through 11 is comparable to Ericson's stages, based on its foraminiferal assemblages and the "*menardii-tumida* complex." The absolute age adopted from Briskin and Berggren (1975) and the nannoplankton zonation by J. Bergen (this volume) plus the absolute ages published by Gartner (1977) are rather inconsistant. Reasons for this inconsistency are (1) irregularly spaced sampling, and (2) questionable nannofossil zonation (missing marker species)—see Bergen (this volume).

Furthermore, extrapolation of absolute age data and the sedimentation rate suggest the Brunhes/Matuyama boundary has to be placed in the lower part of Stage T at Site 541. However, the position of stage boundary U/V, Samples 541-5-1, 108–110 cm and 541-5-2, 17–19 cm, in the middle of the *P. lacunosa* Zone is questionable. Since Bergen (this volume) did not find any *Gephyrocapsa oceanica* below Section 541-1,CC he assigned cores below Section 541-1,CC to the early Pleis-

Table 8. Corresponding ash layers of samples from Holes 541 and 543[a].

Hole 541, Tectonic Unit A (core-section, level in cm)	Hole 541 Tectonic Unit B (core-section, level in cm)	Hole 543 (core-section, level in cm)
16-5, 140	33-3, 135	7-3, 115
18-1, 140 and 20-1, 105	34-5, 75	8-2, 10
18-2, 135 and 20-2, 80	34-6, 50	8-2, 90

[a] Based on data from J. Natland (personal communication, 1982).

tocene. This means that the presence of Stages U and V is questionable, and Stage T may reach up to the top of Core 2. However, the early/late Pleistocene boundary has to be placed in the lower Stage T, somewhere in the interval between Cores 6 and 2. This gives us a sedimentation rate of 100 m/Ma, which seems to be too high. In addition, the "*menardii-tumida* complex" indicates more changes in the water-mass system than Stage T should show. Thus a definite interpretation of Cores 1 through 5 is not possible owing to drilling disturbance.

Pliocene

The early Pliocene of Site 541 is characterized by a fault repetition, based on the nannoplankton age of Sample 541-20-1, 45–46 cm, which is obviously younger than Section 541-19,CC. Wilson (this volume) correlates Section 541-18-3 with Section 541-20-5 on the basis of magnetic data alone. Both sections would correspond to the first normal event in the Gilbert reversed epoch (Cochiti event, 3.72–4.0 Ma). This correspondence agrees very well with the extinction of *G. nepenthes*, which belongs to the "resistant group." This fact is very important, because the occurrence of *G. nepenthes* is rather independent of dissolution, and it is still present in poorly preserved assemblages. If we compare these two datum levels (the Cochiti magnetic event, and the *G. nepenthes* extinction) with the nannofossil boundaries of CN11a and CN10c, we may conclude that the boundary repetitions should be drawn above Sections 541-18-3, and 541-20-5, and not below. The same is true for Tectonic Unit B, Core 34, where *G. margaritae* becomes extinct around Sample 541-34-4, 145–147 cm and *G. nepenthes* in 541-34,CC. Another helpful stratigraphical tool is supplied by comparisons of ash layers (J. Natland, personal communication, 1982), which results in the stratigraphical correlation demonstrated in Table 8.

Annotated Species List

Globigerina falconensis (Blow)

This species is rather rare throughout the Pleistocene at both sites and indicates an influence of temperate water.

Globigerina nepenthes Todd

G. nepenthes occurs in most of the badly preserved samples from Sample 541-18-5, 140–142 cm downward; it is accompanied by *S. dehiscens* and *S. paenedehiscens*. In addition, this species develops a calcite crust, indicating a medium- to deep-water habitat, which would imply that *G. nepenthes* did not have any symbionts. Therefore we placed *G. nepenthes* in the solution susceptibility rank 7.

Globigerinella aequilateralis (Brady)

G. aequilateralis is rare in most cores; even core-top samples from a water depth of 320 m off Barbados contain only 2.2%, which agrees with the living population around Barbados (R (rank factor) = 3).

Globigerinoides conglobatus (Brady)

Compared with other spinose species of the genus *Globigerinoides, G. conglobatus* developes a calcite crust (Bé and Hemleben, 1970; Hemleben et al., 1977). Therefore, it outlasts the rapid increase of dissolution below the lysocline and occurs together with the more resistant groups of the globorotalids, *P. obliquiloculata, S. dehiscens*, and the neogloboquadrinids.

Globigerinoides ruber (d'Orbigny)

G. ruber occurs in several varieties: (1) *G. ruber* (var. pink) and (2) *G. ruber* (var. white), (3) forms with low apertures and thick walls, (4) forms with high-arched apertures and rather thin walls, and (5), the so-called "bottom-variety" (Christiansen, 1965)—the grapelike form (*G. ruber pyramidalis* and *G. ruber elongatus*) that occurs rather often in well-preserved samples. In addition, *G. obliquus* and *G. ruber* seem to be linked by a continuous transition leading to more compact forms, which are more resistant than the other varieties.

In time, *G. ruber* (var. pink) looses its pigment and becomes white. The last observed specimen of *G. ruber* (pink) occurred in Sample 541-7-6, 6–8 cm, which may have been deposited by a gravity flow.

G. ruber, as a surface dweller, reflects in its isotopic composition the changes in the uppermost part of the water column, even more than *G. sacculifer* (Deuser et al., 1981). The latter species inhabits the same environment as *G. ruber*, but its maximum occurrence lies below that of *G. ruber*. Therefore, *G. ruber* reflects water-surface conditions more accurately.

Globigerinoides sacculifer (Brady)

G. sacculifer belongs, like *G. ruber*, to the less-resistant group (R = 4). However, samples with a rather high FDX may contain a remarkable amount of *G. sacculifer*, which can be explained in two ways. One possibility is that the wall thickens as a result of gametogenesis, just prior to gamete release. The last calcification takes place, forming a thin-walled last chamber (Kümmerform or saclike chamber) and/or thickening the whole test with a new layer. This last layer may constitute up to 38% of the wall thickness, according to Bé (1980). Second explanation is that *G. sacculifer* occurs in different varieties. Specimens with a rather low-arched aperture and three chambers in the last whorl are relatively thick-shelled and resemble very much the prefinal stage (beginning of the smooth stage) of *S. dehiscens* (Bé and Hemleben, 1970). This variety is more resistant than the "open" type of *G. sacculifer*.

Another variety of *G. sacculifer*, which we encountered, is *G. fistulosa* (Schubert). This type becomes extinct at the Pliocene/Pleistocene boundary, according to Briskin and Berggren (1975); however, we observed this form throughout the whole section. In our cultures at the Bellairs Laboratory (Barbados) we observed a few specimens of this questionable subspecies.

Globorotalia crassaformis (Galloway and Wissler)

This species is rather rare throughout all cores.

Globorotalia inflata (d'Orbigny)

G. inflata is very rare during the Pleistocene, indicating a temperate water influence during the "glacial" intervals. *G. inflata* never exceeds more than 3% of the total assemblage, with one exception (12%) in Sample 541-9-6, 25–27 cm.

Globorotalia margaritae Bolli and Bermudez and related species: *G. praehirsuta* Blow *G. hirsuta* (d'Orbigny) *G. scitula*

G. margaritae and *G. praehirsuta* never exceed more than 3% of the total assemblage. Their last occurrence appears to be in Sample 541-16-3, 145–147 cm. Not one single specimen of *G. hirsuta* has been found in the Pleistocene samples. In contrast, *G. scitula* occurs throughout the cores, but never exceeds more than 0.5%.

Globorotalia menardii (d'Orbigny) and related species: *G. menardii flexuosa* (Koch) *G. miocenica* Palmer *G. multicamerata* Cushmann and Jarvis *G. tumida* (Brady)

Specimens of these species occur with thin as well as thick walls; especially *G. tumida* and *G. menardii* tend to secrete a thick calcite crust (Hemleben et al., 1977). However, the majority of the Pliocene–Miocene species remains rather thin-walled.

Experiments we performed at the Bermuda Biological Station show that globorotalids (e.g., *G. truncatulinoides, G. inflata*) secrete calcite crusts below approximately 10°C. This information is in good agreement with the isotopic data (Berger, 1979b) and stresses the fact that recent globorotalids spend most of their life below the photic zone, as none of them possesses photosynthesizing symbionts.

Globorotalia truncatulinoides (d'Orbigny) and *G. tosaensis* Takayanagi and Saito

This typical deep-water species occurs alternately with the "*menardii-tumida* complex," indicating mostly "glacial" intervals. *G. truncatulinoides* is normally heavily encrusted with a crystalline calcite crust

(see *G. menardii*). However, it seems to be one rank less resistant than *G. tumida* or the heavily encrusted specimens of *G. menardii*.

The Pliocene/Pleistocene boundary has been defined by the first occurrence of *G. truncatulinoides* in Sample 541-11-4, 131–133 cm, one section below the boundary defined by nannofossils. The co-occurrence of *G. truncatulinoides* and *G. tosaensis* in Sections 541-10,CC through 541-12,CC is in good agreement with the observations published by Brunner and Keigwin (1981).

Hastigerina pelagica (d'Orbigny)

Not one specimen of this thin-walled, tropical to subtropical species has been found. The major reason for this observation lies in the fact that *H. pelagica* destroys its test while undergoing gametogenesis; all chamber septa will be resorbed, sometimes even chamber walls, thus becoming a highly fragile test. At the final stage of gametogenesis, the gamete release happens explosively, often breaking the test totally. Therefore, mostly fragments of this species reach the seafloor (Hemleben et al., 1979) (R = 1)

Neogloboquadrina dutertrei (d'Orbigny) and related species: *N. acostaensis acostaensis* Blow *N. acostaensis humerosa* Takayanagi and Saito

This tropical species, including its ancestors, belongs to the resistant species group. Because *N. dutertrei* s.l. composes up to 30% of the total assemblage, the dissolution rank factor (R = 6) influences highly the FDX of the whole assemblage, especially in well-preserved samples.

Neogloboquardina pachyderma (Ehrenberg)

This species is rather rarely distributed in most "glacial" samples, and never exceeds 3%; all specimens are right-coiled.

Orbulina universa (d'Orbigny)

The sphere of *O. universa* represents the terminal chamber and is usually built 4 to 5 days prior to gametogenesis (C. Hemleben, unpublished data). Most specimens of a tropical population of *O. universa* remain rather thin-walled, although all of them thicken their walls a few hours before gametogenesis. However, some specimens migrate to deeper water and are still calcifying. These specimens "survive" the lysocline dissolution, together with other resistant species.

Pulleniatina obliquiloculata (Parker and Jones)

This subtropical species occurs rather frequently in most well to poorly preserved samples. Its maxima coincide with the minima of the "*menardii-tumida* complex." This phenomenon is difficult to explain, because a dissolution effect can be excluded.

Sphaeroidinella dehiscens (Parker and Jones) and related species: *Sphaeroidinellopsis paenedehiscens* Blow

This species-group is most resistant to dissolution and still occurs in samples in which the calcareous nannofossils are already heavily dissolved. Because dissolution starts inside the test, most of the specimens of samples with a FDX of 7 are hollow. All inner chambers are dissolved, only the outer wall of the last whorl remains.

ACKNOWLEDGMENT

We wish to thank J. C. Moore and B. Biju-Duval (co-chief scientists, Leg 78A) and the crew of the *Glomar Challenger* for the opportunity to participate in Leg 78A and to study the foraminiferal assemblages. Furthermore, we appreciate very much the help provided by I. Breitinger, H. Hüttemann, R. Ott, and W. Wetzel while we prepared the manuscript. We are especially indebted to H. P. Luterbacher, M. Spindler, E. Thomas, and F. Waibel for critically reading the manuscript. We also wish to thank A. Lupke for typing it. Finally, we would like to express our thanks to NSF of the U.S. and the DFG of West Germany for funding the project.

REFERENCES

Adelseck, C. G., Jr., 1978. Dissolution of deep-sea carbonate: preliminary calibration of preservational and morphological aspects. *Deep-Sea Res.*, 24:1167–1185.

Aubouin, J., von Huene, R., et al., 1982. *Init. Repts. DSDP*, 67: Washington (U.S. Govt. Printing Office).

Bé, A. W. H., 1980. Gametogenic calcification in a spinose planktonic foraminifer, *Globigerinoides sacculifer* (Brady). *Mar. Micropaleontol.*, 5:283–310.

Bé, A. W. H., and Hemleben, C., 1970. Calcification in a living planktonic foraminifer, *Globigerinoides sacculifer* (Brady). *N. Jb. Geol. Paläont. Abh.*, 134:221–234.

Berger, W. H., 1968. Planktonic foraminifera: selective solution and paleoclimatic interpretations. *Deep-Sea Res.*, 15:31–43.

_____, 1971. Sedimentation of planktonic foraminifera. *Mar. Geol.*, 11:325–358.

_____, 1973a. Deep-sea carbonates: evidence for a coccolith lysocline. *Deep-Sea Res.*, 20:917–921.

_____, 1973b. Cenozoic sedimentation in the eastern tropical Pacific. *Geol. Soc. Am. Bull.*, 84:1941–1954.

_____, 1975. Deep-sea carbonates: dissolution profiles from foraminiferal preservation. *In* Sliter, W. V., Bé, A. W. H., and Berger, W. H. (Eds.), *Dissolution of Deep-sea Carbonates.* Cushman Found. Foram. Res. Spec. Publ., 13:82–86.

_____, 1979a. Preservation of foraminifera. In *Foraminiferal Ecology and Paleoecology*, SEPM Short Course, 6:105–155.

_____, 1979b. Stable isotopes in foraminifera. In *Foraminiferal Ecology and Paleoecology*, SEPM Short Course, 6:156–197.

_____, 1981. Paleoceanography: the deep-sea record. *In* Emiliani, C. (Ed.), *The Oceanic Lithosphere, The Sea* (Vol. 7): New York (John Wiley and Sons), 1437–1519.

Berger, W. H., Bonneau, M.-C., and Parker, F. L., 1982. Foraminifera on the deep-sea floor: lysocline and dissolution rate. *Oceanol. Acta*, 5:249–258.

Berger, W. H., and von Rad, U., 1972. Cretaceous and Cenozoic sediments from the Atlantic Ocean. *In* Hayes, D. E., Pimm, A. C., et al., *Init. Repts. DSDP*, 14: Washington (U.S. Govt. Printing Office), 787–954.

Berger, W. H., and Winterer, E. L., 1974. Plate stratigraphy and the fluctuating carbonate line. *In* Hsü, K. J., and Jenkins, H. C., (Eds.), *Int. Assoc. Sedimentol., Spec. Publ.*, 1:11–48.

Biju-Duval, G., Mascle, A., Montadert, L., and Wannesson, J., 1978. Seismic investigations in the Colombia, Venezuela and Grenada Basins and on the Barbados Ridge for future IPOD drilling. *Geol. Mijnbouw*, 57:105–116.

Biscaye, P. E., Kolla, V., and Turekian, K. K., 1976. Distribution of calcium carbonate in surface sediments of the Atlantic Ocean. *J. Geophys. Res.*, 81:2595–2603.

Blow, W. H., 1969. Late middle Eocene to Recent planktonic foraminiferal biostratigraphy. *Proc. 1st Int. Conf. Planktonic Microfossils*, Geneva (1967), 1:199–442.

Briskin, M., and Berggren, W. A., 1975. Pleistocene stratigraphy and quantitative paleoceanography of tropical North Atlantic Core V 16-205. In *Late Neogene Epoch Boundaries*, Micropaleontol. Press Spec. Publ., pp. 167–198.

Brunner, C. A., and Keigwin, L. D., Jr., 1981. Late Neogene biostratigraphy and stable isotope stratigraphy of a drilled core from the Gulf of Mexico. *Mar. Micropaleontol.*, 6:397–418.

Christiansen, B. O., 1965. A bottom form of the planktonic foraminifer *Globigerinoides rubra* (D'Orbigny, 1839). *Pub. Staz. Zool. Napoli*, 34:197–202.

CLIMAP, 1976. The surface of the ice age earth. *Science*, 191:1131–1137.

Deuser, W. G., Ross, E. H., Hemleben, C., and Spindler, M., 1981. Seasonal changes in species composition, numbers, mass, size, and isotopic composition of planktonic foraminifera settling into the deep Sargasso Sea. *Palaeogeogr. Palaeoclimatol. Palaeoecol.*, 33: 103–127.

Ericson, D. B., and Wollin, G., 1968. Pleistocene climates and chronology in deep-sea sediments. *Science*, 162:1227–1234.

Gartner, S., 1977. Calcareous nannofossil biostratigraphy and revised zonation of the Pleistocene. *Mar. Micropaleontol.*, 2:1–25.

Hemleben, C., Bé, A. W. H., Anderson, O. R., and Spindler, M., 1979. "Dissolution" effects induced by shell resorption during gametogenesis in *Hastigerina pelagica* (D'Orbigny). *J. Foram. Res.*, 9:118–124.

Hemleben, C., Bé, A. W. H., Anderson, O. R., and Tuntivate, S., 1977. Test morphology, organic layers and chamber formation of the planktonic foraminifer *Globorotalia menardii* (D'Orbigny). *J. Foram. Res.*, 7(1):1–25.

Hussong, R. M., Uyeda, S., et al. 1982. *Init. Repts. DSDP*, 60: Washington (U.S. Govt. Printing Office).

Moore, J. C., Biju-Duval, B., et al., 1982. Offscraping and underthrusting of sediment at the deformation front of the Barbados Ridge: Deep Sea Drilling Project Leg 78A. *Geol. Soc. Am. Bull.*, 93:1065–1077.

Okada, H., and Bukry, D., 1980. Supplementary modification and introduction of code numbers to the low-latitude coccolith biostratigraphic zonation (Bukry 1973, 1975). *Mar. Micropaleontol.*, 5: 321–325.

Parker, F. L., and Berger, W. H., 1971. Faunal and solution patterns of planktonic foraminifera in surface sediments of the South Pacific. *Deep-Sea Res.*, 18:73–107.

Schnitker, D., 1979. Cenozoic deep water benthic foraminifers, Bay of Biscay. *In* Montadert, L., Roberts, D. G., et al., *Init. Repts. DSDP*, 48: Washington (U.S. Govt. Printing Office), 377–414.

Schott W., 1935. Die Foraminiferen in dem äquatorialen Teil des Atlantischen Ozeans. *Deut. Atlant. Exped. Meteor 1925–1927*, 3: 43–134.

Shackleton, N. J., and Opdyke, N. D., 1977. Oxygen isotope and paleomagnetic evidence for early Pliocene northern hemisphere glaciation. *Nature*, 270:216–219.

Sliter, W. V., Bé, A. W. H., and Berger, W. H. (Eds.), 1975. *Dissolution of Deep-Sea Carbonates*. Cushman Found. Foram. Res. Spec. Publ., 13:159.

Stainforth, R. M., Lamb., J. L., Luterbacher, H., Beard, J. H., and Jeffords. R. M., 1975. Cenozoic planktonic foraminiferal zonation and characteristics of index forms. *Univ. of Kansas, Paleontol. Contribs., Art. 62.*

Steven, D. M., and Brooks, A. L., 1972. Identification of Amazon River water at Barbados, West Indies, by salinity and silicate measurements. *Mar. Biol.*, 14:345–348.

Thunnell, R. C., and Honjo, S., 1981. Calcite dissolution and the modification of planktonic foraminiferal assemblages. *Mar. Micropaleontol.*, 6:169–182.

Tomblin, J. F., 1975. The Lesser Antilles and Aves Ridge. *In* Nairn, A., and Stehli, F. G. (Eds.), *The Ocean Basins and Margins* (Vol. 3): New York (Plenum Press), 1–64.

van Donk, J., 1976. 0-18 record of the Atlantic Ocean for the entire Pleistocene epoch. *In* Cline, R. M., and Hays, J. D. (Eds.), *Investigations of Late Quaternary Paleoceanography and Paleoclimatology*, Geol. Soc. Am. Mem., 145:147–163.

von Huene, R., Nasu, N., et al., 1980. *Init. Repts. DSDP*, 56, 57, pt. 2: Washington (U.S. Govt. Printing Office).

Watkins, J. S., Moore, J. C., et al. 1982. Init. *Repts. DSDP*, 66: Washington (U.S. Govt. Printing Office).

Date of Initial Receipt: March 14, 1983
Date of Acceptance: September 21, 1983

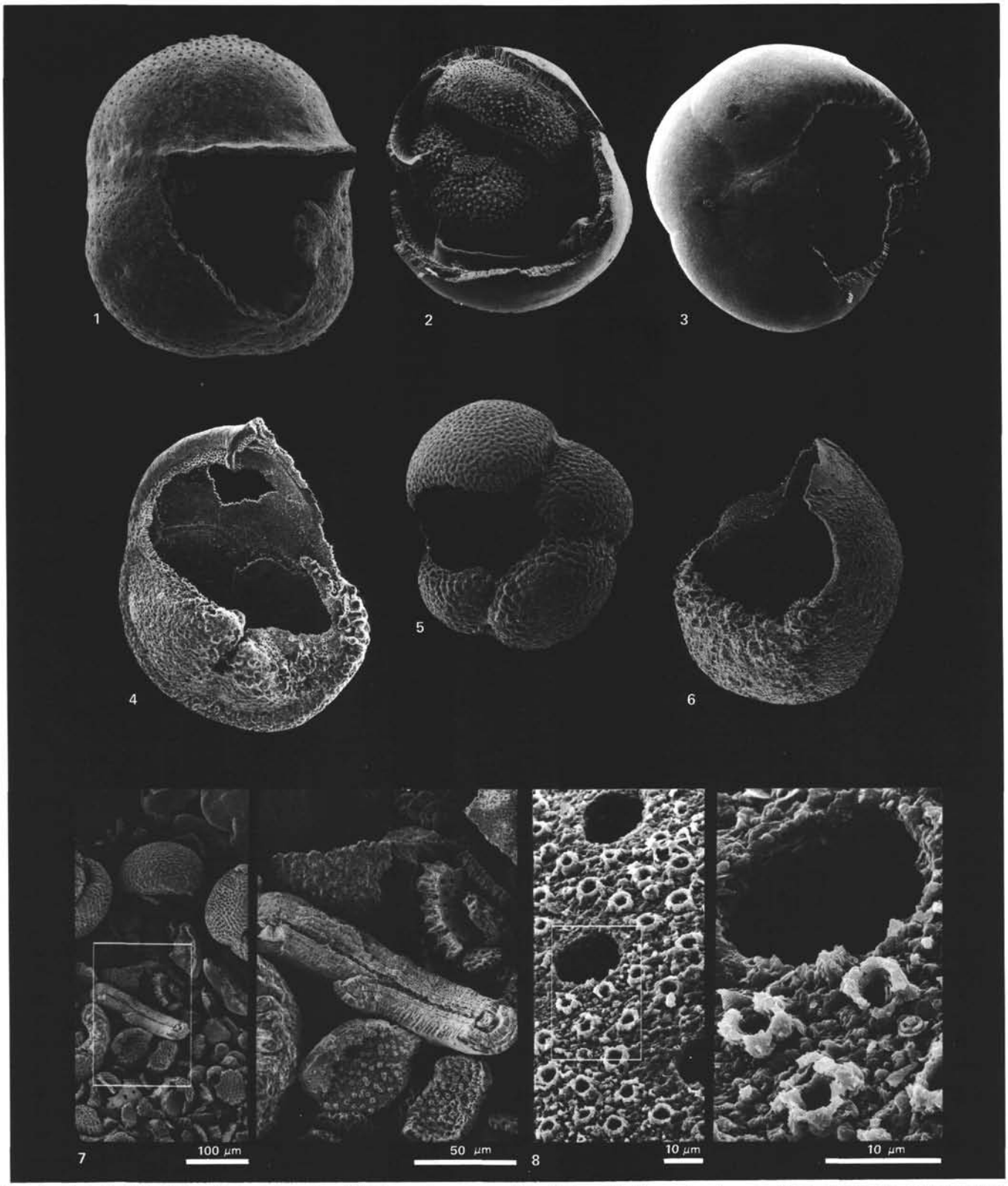

Plate 1. **1–6.** Umbilical view of selected species exhibiting various stages of dissolution. Most inner chambers are dissolved; only the outside wall of the last whorl remains. All figures are the umbilical views and are magnified ×85. (1) *Spaeroidinella dehiscens* (Parker and Jones). Sample 541-3,CC. (2) *Pulleniatina obliquiloculata* (Parker and Jones). Sample 541-16-3, 145–147 cm. (3) *Pulleniatina obliquiloculata* (Parker and Jones). Sample 541-3,CC. (4) *Globorotalia menardii* (d'Orbigny). Sample 541-2-1, 27–29 cm. (5) *Neogloboquadrina dutertrei* (d'Orbigny). Sample 541-2-3, 127–129 cm. (6) *Globorotalia truncatulinoides* (d'Orbigny) Sample 541-2-3, 127–129 cm. **7.** Chamber and keel fragments from Sample 541-15-3, 17–19 cm. **8.** Chamber fragments exhibiting pore funnels, a typical result of dissolution; from Sample 541-17-6, 32–34 cm.

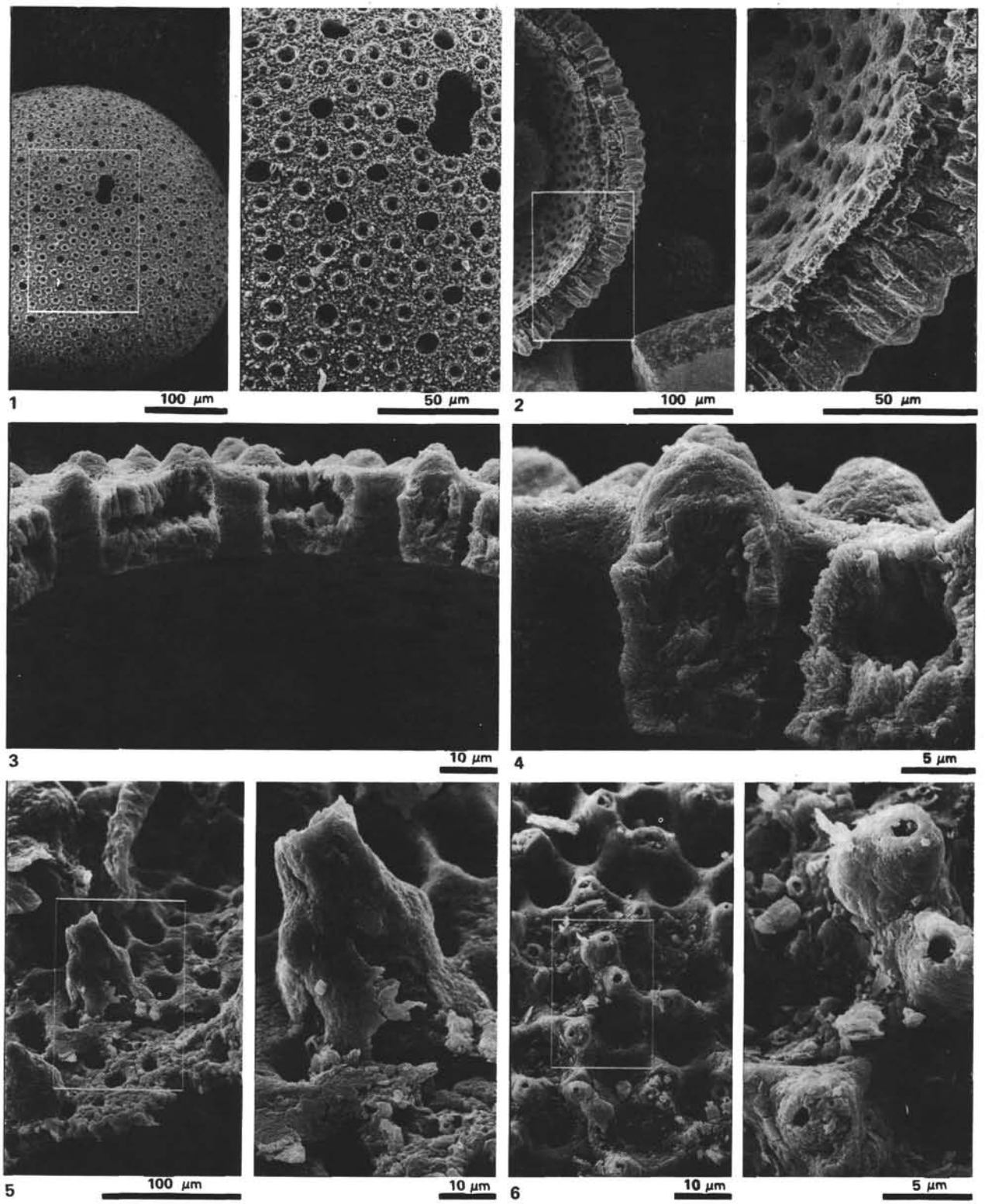

Plate 2. **1–4.** Pore widening and wall destruction in *Orbulina universa* (d'Orbigny), showing that dissolution destroys the wall from the inside. (1) *O. universa* (d'Orbigny) from Sample 541-4-6, 117–119 cm. (2) *O. universa* (d'Orbigny) from Sample 541-15-3, 17–19 cm. (3–4) *O. universa* (d'Orbigny) from Sample 541-8-5, 19–21 cm. **5.** *Globorotalia menardii* (d'Orbigny) showing the lamellar construction of the pustules as a result of dissolution. Sample 541-2-1, 27–29 cm. **6.** *Globigerinoides ruber* (d'Orbigny) showing spine holes resulting from resorption during gametogenesis. Sample 541-3-2, 46–48 cm.

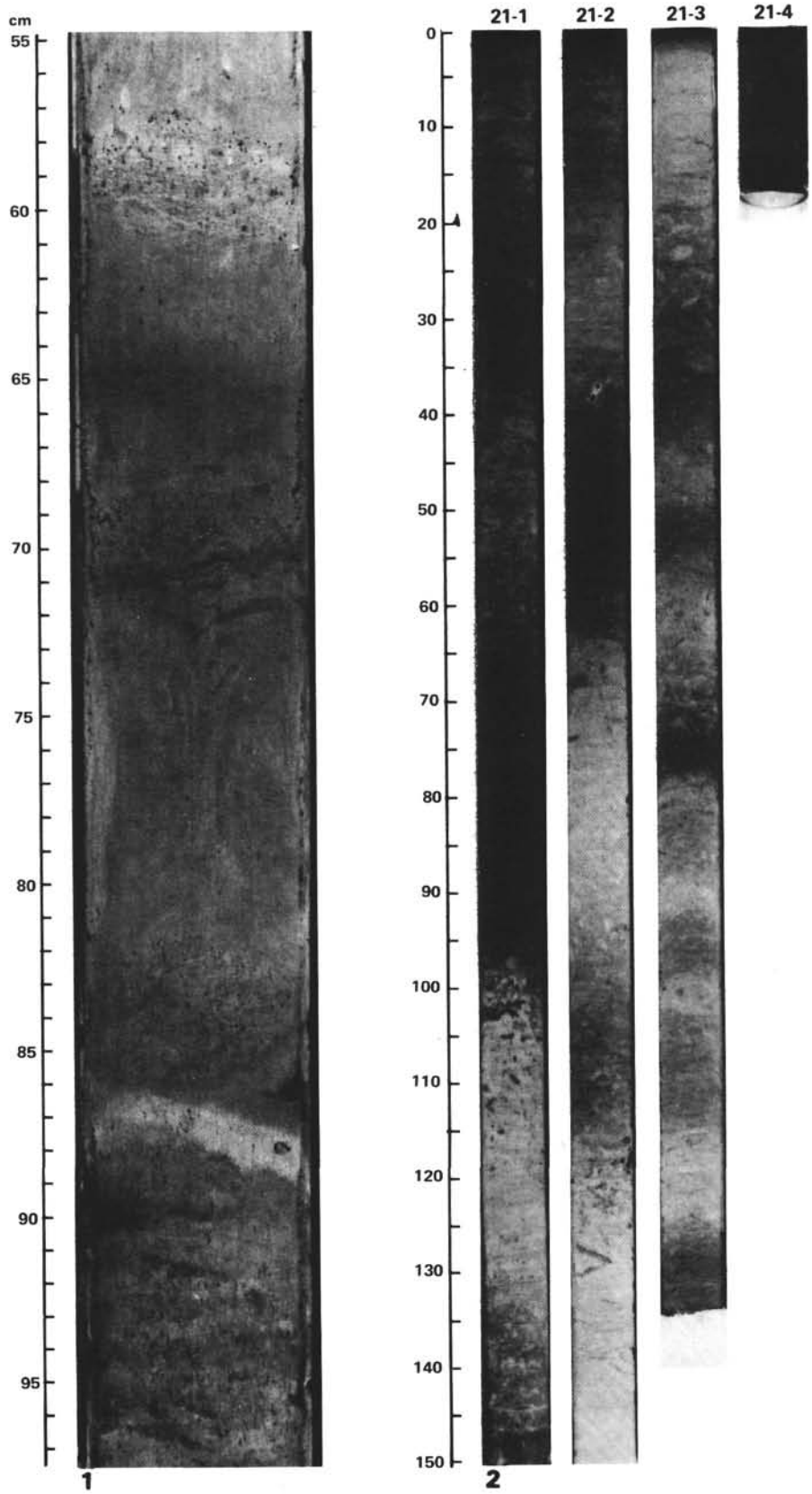

Plate 3. **1.** Sample 541-13-6, 55–97 cm exhibits three gravity flows at 59, 70, and 85 cm. **2.** Core 541-21, showing sediment totally mottled by bioturbation; the dark (poor in carbonate) and light (rich in carbonate) alternating layers may be interpreted as reflections of climatic fluctuations.